
Masters Theses

Student Theses and Dissertations

Fall 2017

Quantifying ceramic proppant transport in complex fracture networks

Vivekvardhan Reddy Kesireddy

Follow this and additional works at: https://scholarsmine.mst.edu/masters_theses



Part of the [Petroleum Engineering Commons](#)

Department:

Recommended Citation

Kesireddy, Vivekvardhan Reddy, "Quantifying ceramic proppant transport in complex fracture networks" (2017). *Masters Theses*. 7720.

https://scholarsmine.mst.edu/masters_theses/7720

This thesis is brought to you by Scholars' Mine, a service of the Missouri S&T Library and Learning Resources. This work is protected by U. S. Copyright Law. Unauthorized use including reproduction for redistribution requires the permission of the copyright holder. For more information, please contact scholarsmine@mst.edu.

QUANTIFYING CERAMIC PROPPANT TRANSPORT IN COMPLEX
FRACTURE NETWORKS

by

VIVEKVARDHAN REDDY KESIREDDY

A THESIS

Presented to the Faculty of the Graduate School of the
MISSOURI UNIVERSITY OF SCIENCE AND TECHNOLOGY

In Partial Fulfillment of the Requirements for the Degree

MASTER OF SCIENCE IN PETROLEUM ENGINEERING

2017

Approved by

Shari Dunn-Norman, Advisor
Abdulmohsin Imqam, Co-Advisor
Larry K Britt
Baojun Bai

© 2017

Vivekvardhan Reddy Kesireddy

All Rights Reserved

ABSTRACT

Water fracs have become an essential part of unconventional reservoirs to create deeper fracture networks. Proppant transport in water fracs is challenging in terms of fluids ability to carry the proppant deeper into these fracture networks. This experimental study investigates the impact of the flow rates, fracture widths and complexity controlling the ability of proppant to flow into complex fracture networks. This research attempts to nullify the knowledge gap in understanding width heterogeneity in primary and secondary fractures. This study speaks for settling pattern and proppant transport through a slot flow model with a unique approach to understand stage wise distribution of proppant. The slurry was injected in multiple fracture pore volumes at required flow rates to monitor the stage-wise development of proppant bed. Study illustrates proppant transport in terms of proppant bed heights, equilibrium dune levels and proppant area fractions. Results represents proppant transport for fracture widths, which are comparable to proppant diameter. Two different configurations of apparatus were used to investigate heterogeneity in width in complex fracture networks. Results describe stepwise distribution of ceramic proppant under the influence of flow rates, fracture width and complexity. The bed height gradually builds up in the slot with each injection to achieve an equilibrium bed height. Injection slurry velocities primarily affect proppant transport affecting its distribution in fractures. The fracture width showed a significant impact on proppant transport. Width heterogeneity in complex fracture systems provide better proppant distribution in complex fracture networks. Heterogeneity of width in the fracture caused increased settling and more proppant surface area fractions. The results help in optimizing the proppant flow patterns into complex fracture networks.

ACKNOWLEDGMENTS

I express my heartfelt gratitude and earnest appreciation: To Dr. Shari Dunn-Norman, my guide and advisor, who was kind enough to provide me an opportunity to carry out this study, for her invaluable guidance and financial support which empowered me to this eventful outcome without any impediments. She has been an incredible person and I take immense pleasure in being her student. I hope to remain one all my future.

To Dr. Imqam who has been an immense support system, helping me through all the critical phases for this study. He has been a guiding force and his advice at all junctures during the study which enabled me to accomplish this work to my level best.

To Professor Britt who gave me critical suggestions to carry forward this study in a better way and Dr. Bai for his conitnous support through this journey.

A special thanks to Jeff Heniff from Rock Mechanics department for his guidance and support. I would also like to thank my friends and lab mates, and faculty and staff of the department of petroleum engineering for their support, suggestions and constant appreciation.

Words fail to convey my love and gratitude for the moral support extended by my family and their unconditional love which is priceless and inexpressible.

TABLE OF CONTENTS

	Page
ABSTRACT.....	iii
ACKNOWLEDGMENTS	iv
LIST OF ILLUSTRATIONS.....	viii
LIST OF TABLES.....	xi
NOMENCLATURE	xii
 SECTION	
1. INTRODUCTION.....	1
1.1. FRACTURING FLUID SELECTION.....	7
1.2. PROPPANT SELECTION.....	8
1.3. IMPORTANCE OF QUANTIFYING PROPPANT TRANSPORT.....	10
1.4. MOTIVATION	15
1.5. RESEARCH OBJECTIVES.....	16
1.6. RESEARCH SCOPE.....	16
2. LITERATURE REVIEW AND BACKGROUND.....	18
2.1. PROPPANT TRANSPORT IN CROSSLINKED FLUIDS	19
2.2. PROPPANT TRANSPORT IN NON-VISCOUS FLUIDS.....	21
2.3. FACTORS INFLUENCING PROPPANT TRANSPORT	24
2.3.1. Fluid Flow Properties.....	25
2.3.1.1. Effect of pump flow rates	27

2.3.2.	Proppant Properties.....	28
2.3.2.1.	Effect of proppant size on proppant transport.....	28
2.3.2.2.	Effect of proppant concentration.	30
2.3.3.	Effect of Fracture Complexity.	31
3.	EXPERIMENTAL DESCRIPTION AND PROCEDURE.....	34
3.1.	EXPERIMENTAL APPARATUS.....	34
3.1.1.	Primary Fracture.	34
3.1.2.	Primary and Secondary Fracture.....	37
3.2.	EXPERIMENTAL DESCRIPTION	41
3.3.	EXPERIMENTAL PROCEDURE.....	43
4.	RESULTS AND ANALYSIS	46
4.1.	RESULTS FOR PRIMARY FRACTURES.....	46
4.1.1.	Effect of Flow Rate on Proppant Transport.....	46
4.1.2.	Effect of Fracture Width on Proppant Transport.....	53
4.1.3.	Understanding Proppant Transport for W/D Ratio Less than 2.5.....	58
4.1.4.	Conclusions for Primary Fractures.	61
4.2.	RESULTS FOR SECONDARY FRACTURES	62
4.2.1.	Effect of Changing the Width of Primary Fracture.	63
4.2.2.	Effect of Primary Fracture Width Heterogeneity.....	67
4.2.3.	Conclusions for Secondary Fracture Apparatus.	73
4.3.	PARTICLE SIZE DISTRIBUTION ANALYSIS.....	74
5.	CONCLUSIONS.....	80

6. FUTURE WORK.....	81
6.1. EFFECT OF PROPPANT SPHERICITY/SHAPE	81
6.2. EFFECT OF FRACTURE WIDTH HETEROGENEITY	81
6.3. PARTICLE SIZE DISTRIBUTION	82
6.4. MULTIPLE PROPPANT SIZES	82
6.5. USING DIFFERENT FLUIDS WITH CURRENT APPROACH.....	83
APPENDIX.....	84
REFERENCES	87
VITA	91

LIST OF ILLUSTRATIONS

	Page
Figure 1.1. U.S. shale production (billion cubic feet).....	1
Figure 1.2. Sand build-up in a fracture	3
Figure 1.3. Schematic of sand transport in a vertical planar fracture	3
Figure 1.4. Conductivity as a result of effective stresses on proppant.	4
Figure 1.5. Relationship between relative capacity parameter and effective well radius....	5
Figure 1.6. Cinco ley relation for effective wellbore radius	6
Figure 1.7. Proppant conductivity pyramid showing three tiers of proppant.	10
Figure 1.8. Research scope	17
Figure 2.1. Settling velocity corrected to inertial effects.....	23
Figure 2.2. Particle reynolds number as a function of radius	23
Figure 2.3. Force acting on a proppant particle entering a fracture slot	26
Figure 2.4. Settling rate for various proppant sizes	29
Figure 2.5. Correlations to study the effect of concentration on settling velocities	31
Figure 3.1. Comparison of primary and secondary configurations of the apparatus.....	34
Figure 3.2. Plexi glass setup for primary configurations of the apparatus.	35
Figure 3.3. Experimental setup with the parallel plate apparatus	36
Figure 3.4. Secondary fracture apparatus setup.	38
Figure 3.5. Plexi glass setup for apparatus with primary and secondary fractures.....	38
Figure 3.6. Schematic with primary and secondary fractures.....	39
Figure 3.7. 3 different cases for experiments in primary and secondary fractures	40
Figure 3.8. Measurement of heights at various points within fracture slots	45

Figure 4.1. Development of sand dune heights as it reaches equilibrium.	47
Figure 4.2. Proppant distribution at end of FPV 1 for different flow rates.....	48
Figure 4.3. Effect of flow rates on proppant transport in terms of bed height.....	49
Figure 4.4. Comparison of bed heights for different flow rates at equilibrium	50
Figure 4.5. Comparison of equilibrium dune level (for different flowrates)	50
Figure 4.6. Comparison of bed heights at equilibrium	51
Figure 4.7. Surface area fraction of proppant for different flow rates.	52
Figure 4.8. Effect of flow rates in terms of fracture pore volume injections.....	53
Figure 4.9. Proppant distribution at end of FPV 1 for different widths ($W/D \sim 3$)	54
Figure 4.10. Proppant distribution at end of FPV 1 for different widths ($W/D > 3$)	55
Figure 4.11. Comparison of bed heights at end of FPV 1 for different widths	56
Figure 4.12. Comparison of EDL bed heights for various frac widths.....	56
Figure 4.13. Equilibrium dune levels for various W/D ratios.....	57
Figure 4.14. Effect of fracture width in terms of fracture pore volume injections	58
Figure 4.15. Fracture slot showing proppant unable to transport for W/D ratio of 1.18 ...	59
Figure 4.16. Fracture slot showing proppant transport ability for W/D ratio of 2.28.....	60
Figure 4.17. Surface area fraction covered by proppant for different fracture widths	60
Figure 4.18. Apparatus setup for case 1 and case 2 (top view)	63
Figure 4.19. Proppant bed at end of FPV 1 (primary slot) case 1 vs case 2	64
Figure 4.20. Proppant bed at end of FPV 1 (secondary slot) case 1 vs case 2.....	65
Figure 4.21. Proppant bed heights at equilibrium in primary slot (case1 Vs case2)	66
Figure 4.22. Proppant bed heights at equilibrium in primary slot (case 1 vs case 2)	66
Figure 4.23. Comparison of equilibrium dune levels in primary and secondary slots	67

Figure 4.24. Apparatus setup for case 1 and case 3 (top view)	68
Figure 4.25. Proppant bed at end of FPV 2 (primary slot) for case 1 and case 3	69
Figure 4.26. Proppant bed at end of FPV 2 (secondary slot) for case 1 and case3	70
Figure 4.27. Comparison of proppant bed heights in primary slot (case 1 vs case 3)	70
Figure 4.28. Comparison of proppant bed heights in secondary slot (case 1 vs case 3)....	71
Figure 4.29. EDL bed heights in primary and secondary slots (case 1 Vs case 3)	71
Figure 4.30. Surface area fraction for primary slots (case 1, case 2 and case 3)	72
Figure 4.31. Surface area fraction for secondary slot (case 1 , case 2 and case 3)	73
Figure 4.32. Particle size distribution analysis	74
Figure 4.33. Example of results obtained from particle size analyser	76
Figure 6.1. Proppant settling with high and low sphericity	81
Figure 6.2. Study of heterogeneity in fracture width for complex fracture networks	82

LIST OF TABLES

	Page
Table 2.1. Recent literature on slickwater facturing (experimental and CFD).....	22
Table 3.1. Parameters used to study the effect of flow rates on proppant transport.....	41
Table 3.2. Parameters to study the effect of fracture widths on proppant transport.....	42
Table 3.3. Parameters used to study the effect of fracture complexity.....	43
Table 4.1. Results for particle size distribution analysis (D50) for Case 1	77
Table 4.2. Summary of results for particle size analysis	78
Table 4.3. Reference terminology for particle distribution.....	79

NOMENCLATURE

v_s	Particle density, cm/s
g	Gravitational constant, 980 cm/s ²
ρ_p	Particle density, gm/cc
ρ_f	Fluid density, gm/cc
d_p	Particle diameter, cm
μ_f	Fluid viscosity, poise
α, β	Boundary layer coefficients
$V_{equilibrium}$	Equilibrium velocity, ft/min
Q	Injection rate, bbl/min
W	Fracture width, in
h_o	Cross-sectional area above-settled sand, ft
C_{fD}	Dimensionless fracture conductivity
k_f	Fracture permeability, md
W	Fracture width, ft
k	Reservoir permeability, md
x_f	Fracture half length, ft
θ	Angle of repose
l	Fracture length, mm
h	Fracture height, mm
v_w	Settling rate corrected for presence of walls, cm/s
v_s	Settling rate of particle in Stokes flow, cm/s
a	Particle radius, cm

l	Fracture wall thickness, cm
P	Pressure,
ρ	Slurry density, m/cc
m_p	Proppant mass, gm
m_w	Water mass, gm
V_p	Proppant volume, cc
V_w	Water volume, cc
g	Acceleration due to gravity, 980.6 cm/s ²
v	Slurry horizontal velocity, ft/s
K_L	Loss coefficient, dimensionless
d	Smaller diameter pipe, cm
D	Bigger diameter pipe, cm
D_e	Equivalent diameter, cm
h	Slot height, cm
w	Slot width, cm
μ	Slurry viscosity, poise
Q_s	Slurry flowrate, cm ³ /s
l	Slot length, cm
V_\emptyset	Settling rate of concentrated particle, cm/s
\emptyset	Proppant concentration (Volume of solid/Volume of mixture)

1. INTRODUCTION

An increasing demand for oil and gas, coupled with declining production from conventional oil and gas fields, led to the exploration and development of unconventional reservoirs, previously thought to be source rock. Over the past decade, advances in multi-stage horizontal fracturing and completion methods enabled commercial development of many shale reservoirs. Accordingly, US shale production has seen a significant rise in production from 1.2 TCF in 2007 to 15.2 TCF IN 2015 according to the U.S. Energy Information Administration (in Figure 1.1).

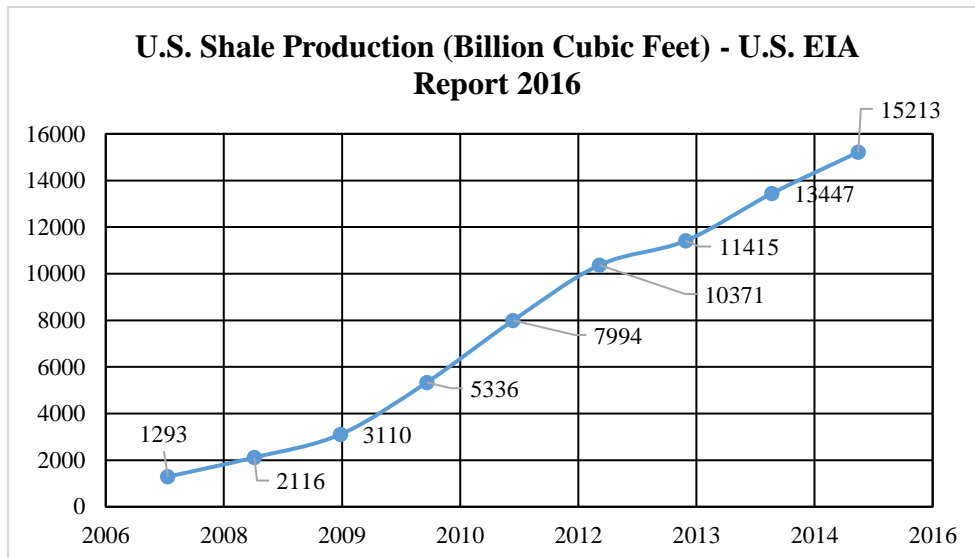


Figure 1.1. U.S. shale production (billion cubic feet) (EIA report 2016)

Reservoirs having low permeability i.e. less than .01 md are widely classified as unconventional. Hydraulic fracturing plays a significant and critical role in the commercial development of these kinds of reservoirs. The primary objective of hydraulically fracturing is to establish greater and wider reservoir drainage contact area,

or stimulated reservoir volume (SRV), which also connects and drains existing fractures in the shale matrix.

There are many design factors in hydraulic fracturing, such as pump rate, pressure, fluid type, fluid viscosity, and proppant type, size and concentration. The combination of these treatment design factors, coupled with the formation type, rock type and geomechanical properties, affect the overall fracture half length, width and height. Design considerations of any hydraulic fracturing process must evaluate creating fracture length (usually referred to as $\frac{1}{2}$ length, x_f or penetration) versus fracture conductivity (K_{fw}), i.e. propped fracture width times the fracture permeability). The contact drainage area created by fracturing is a function of fracture lateral length, height and half-length, and then the number of fractures created. Fracture half-length is determined from the treatment design parameters using numerical modeling. Fracture conductivity, K_{fw} , is another factor that defines the fluid ability to flow through the fracture.

The design of any fracture treatment inevitably requires usage of two basic materials. One is the fluid and other is proppant. Fluid is used for fracture initiation and propagation, and acts as a carrier to transport the proppant into the fracture. Proppant helps in retaining the conductivity of the fracture post release of fluid pressure when the overburden causes closure on created fractures. Hence, material selection is always a major component of both operations/execution and as a part of treatment designs.

Fracture conductivity requirements are pre-estimated in the proppant selection process, as fracture conductivity is controlled by the size of the proppant being used, concentration pumped, and distance to which proppant has been transported into the fracture. Since proppant placement affects proppant conductivity and well flow, proppant transport is an important outcome in a hydraulic fracturing treatment. Figure 1.2 and Figure 1.3 illustrate transport of proppant in a fracture where a slurry of proppant (sand) and fluid are injected. Proppant usually deposits to form a bed before it is actually pushed forward by the incoming injected fluids.

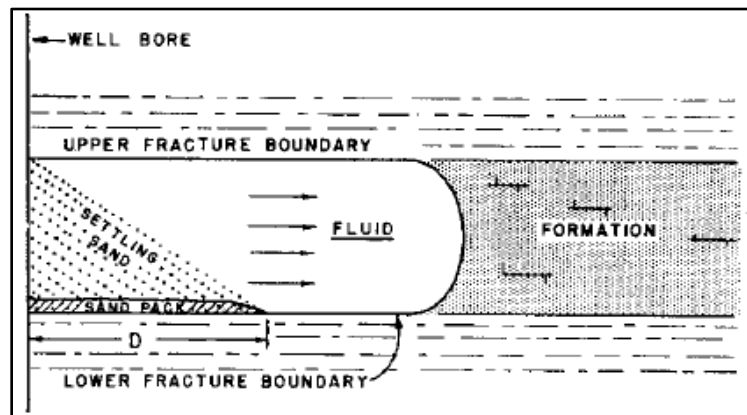


Figure 1.2. Sand build-up in a fracture (Kern et al. 1959)

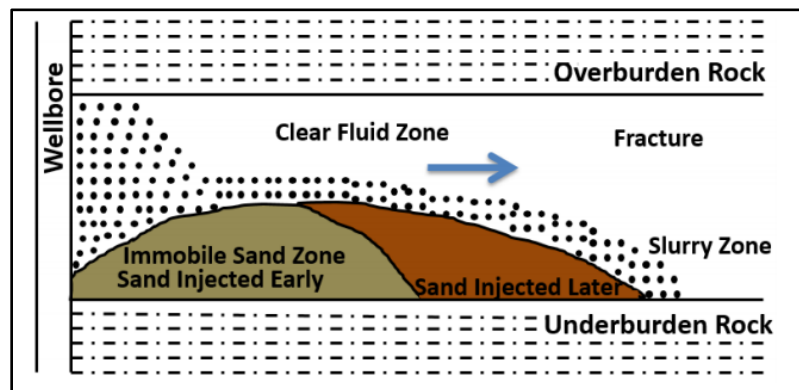


Figure 1.3. Schematic of sand transport in a vertical planar fracture (Mohanty et al. 2016)

As shown in the Figure 1.2 and Figure 1.3, the sand initially settles along the inlet perforations from the wellbore and fluid passes further into the fracture. This fluid is subjected to leak off phenomenon where in the carrier fluid is dissipated into the surroundings leaving the proppant in the fracture. This proppant is subjected to closure stress post release of fluid pressure. The conductivity of proppant drastically reduces after application of closure stress. Figure 1.4 shows the how increasing closure stress degrades fracture conductivity.

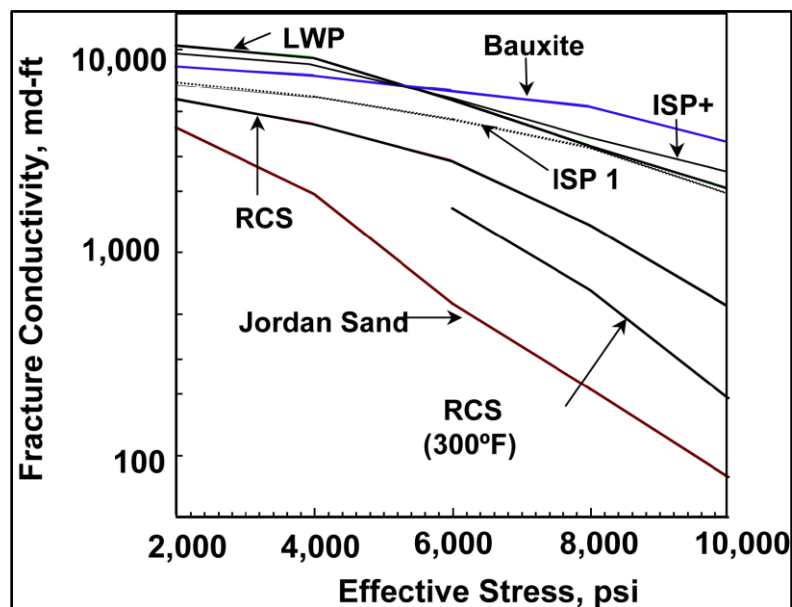


Figure 1.4. Conductivity as a result of effective stresses on proppant

The transport of proppant into the fracture is important, as it affects fracture the propped area of the fracture, and defines where the fracture may not be sufficiently propped. As mentioned above, the conductivity of a fracture is the product of propped fracture width and permeability of propping agent.

Cinco Ley et al. 1981 introduced the term dimensionless fracture conductivity F_{cd} including the terms fracture half-length and width and is given by the equation

$$F_{cd} = \frac{K_f w}{K x_f} \quad (1.1)$$

Dimensionless fracture conductivity is an inverse to the relationship defined by Pratt in 1961. This relationship was between effective wellbore radius and relative capacity parameter, a . Figure 1.5. Shows Pratt's curve where large values of a ($K_f x_f$) imply less effective well radius ($K_f W$). Relative capacity tends to reach a constant value at effective well bore radius of 0.5 and at a relative capacity parameter value of $a = 0.01$.

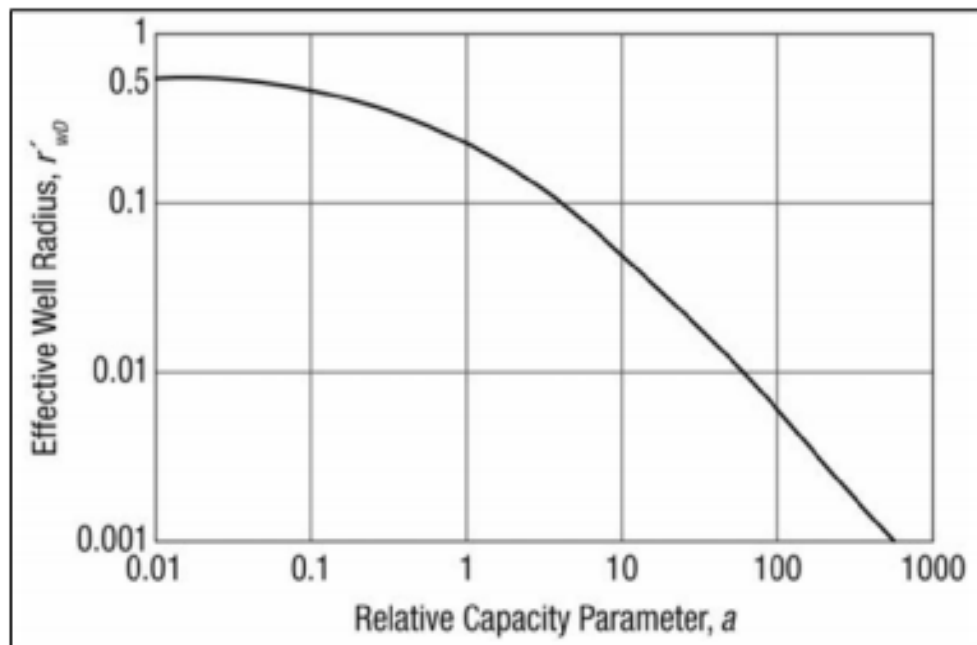


Figure 1.5. Relationship between relative capacity parameter and effective wellbore radius (Economides et al, 2013)

The Cinco-ley correlation can be seen in Figure 1.6, which relates the dimensionless conductivity of the fracture to the equivalent well bore radius and fracture half-length. Usage of effective wellbore radius will help in describing fractures and in reservoir-engineering relations such as calculation of Folds of increase (FOI) (Britt et al. 2009). In addition, it can be proven mathematically that maximum FOI for a given volume of proppant is achieved when F_{cd} is about 2.

For low permeable unconventional reservoirs like shale (usually $K < 0.0001$ md) large half-lengths provide better fracture performance, shown as an infinite conductivity fracture at $F_{cd} > 30$.

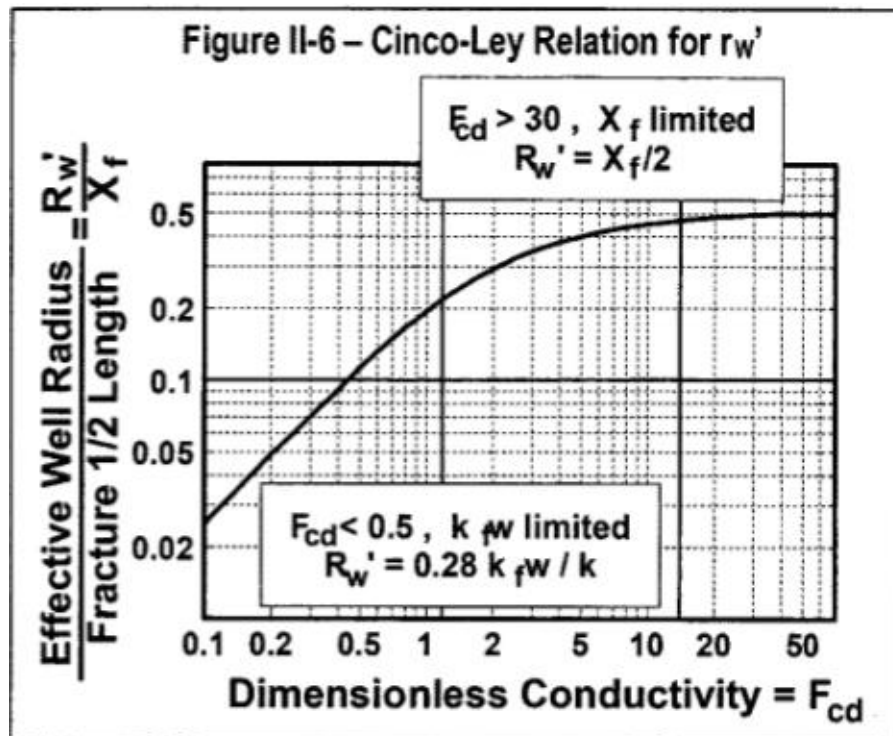


Figure 1.6. Cinco ley relation for effective wellbore radius

Fracture fluid selection and fracture fluid leak off are factors influencing the fluid efficiency, which in turn controls the half length. However, the height of fracture is based on fluid viscosity and stress difference between the pay and surrounding zones.

A brief introduction to fracturing fluid selection and proppant selection will be provided in the following Sections 1.1 and 1.2.

1.1. FRACTURING FLUID SELECTION

As mentioned previously, fracture geometry (half length and fracture height) is directly affected of fracture fluid type, viscosity, and pump rate. The fracturing fluid propagates the fracture by providing the hydraulic pressure to break the rock. The fluid leaks off to the formation in this process, and then also transports the proppant into the fracture. Hence, the selection of fracturing fluid is fundamental in the fracturing design process. Another important characteristic of a fracturing fluid is to be compatible with reservoir fluids, inexpensive and environmentally friendly. Several rheological properties define the selection of fracturing fluids. Viscosity is a factor that can be used to classify fracturing fluids. Slickwater and crosslinked fluids are two broad classifications of fracturing fluids based on viscosity. Fracture stimulation with cross-linked (high viscous fluids) usually provide a greater proppant carrying capacity.

On the other hand, slickwater being low viscous have lower proppant carrying capacity. Nonetheless, each of these types of fluids are used based on the existing conditions for a particular field.

Linear gel and cross-linked viscous fluids have been traditionally used for fracturing treatment in conventional reservoirs to carry larger proppant size particles. Proppant placement problems are reduced to a minimum when using these fluids due to their high proppant carrying capacity. On the other hand, for treatment with low viscous fluids such as slickwater/treated water, smaller proppant sizes can be effective. Such treatments are potentially used in low permeability unconventional reservoirs. Low permeability reservoirs need high fracture half-lengths to maintain an optimum value of dimensionless fracture conductivity. The design of fracturing treatment in low permeability reservoir focuses on creating a more complex fracture network to conductivity since the surface is strongly influenced production.

In low permeability reservoirs, hydraulic fracturing design focuses more on creating deeper fracture networks than conductivity since the hydraulic fracture surface area strongly influences production in these cases. The fracture penetration and geometry will be influenced by the net pressure equation, which will be explained in the proppant selection section along with the design parameters.

1.2. PROPPANT SELECTION

As noted previously, proppant is a solid material, such as sand or ceramic, that is pumped along with the fracturing fluid, to hold the fracture open after pump pressure is released. Proppants vary in size and can be pumped at different concentrations. Proppant cost constitutes a significant portion of a well-treatment cost and the ultimate goal for selecting the right proppant is to maximize the Net Present Value (NPV) for a given well.

Selection of proppant is a major aspect of any fracturing treatments as production increase is a consequence of fracture conductivity, which ultimately depends on the in situ proppant characteristics and closure stress on proppant. As mentioned in Palisch et al. 2012 there are two important considerations for proppant selection, one of them being short term and the other being long term. Short term considerations for any reservoir is clean-up and early production following fracturing where as the long term consideration is the ability to withstand the stress environment as the well produces and reservoir pressure depletes.

There are different types of proppants including sand, bauxite, intermediate – high strength ceramics. Based on its availability and cost, sand is most widely used among them. However, the individual properties define their application in fields. Among these properties, withstanding stress at wellbore along with proppant size and concentration are of primary importance. Higher proppant size provides a greater conductivity; however, this proppant requires higher viscous fluids as a carrier. In conventional reservoirs, conductivity is improved using larger proppant size with little impact on proppant cost. This is true provided the proppant is placed successfully during treatment. Gallagher et al, 2011 provided a classification in the Figure 1.7 based on the conductivity and the respective characteristics of proppant materials used in industry. As you move up the triangle the conductivity increases. Palisch et al. 2012

Wang et al. 2009 has presented modeled comparisons in tight reservoirs based the various conductivity damage mechanisms. Factors such as the multiphase flow of fluids,

proppant crushing at high closure stresses, the yield stress of fracturing liquid and filter cake formation are some of the issues which reduce the conductivity to a smaller fraction of estimated values. Hence, closure stress is an important criterion for proppant selection.



Figure 1.7. Proppant conductivity pyramid showing three tiers of proppant.(Gallagher et al. 2011)

Ultimate proppant transport abilities defines the effective hydraulic length of fracture which contributes to well productivity. The importance this proppant transport is discussed in Section 1.3.

1.3. IMPORTANCE OF QUANTIFYING PROPPANT TRANSPORT

The success of any hydraulic fracturing treatment depends on flow area and permeability of the induced fractures. Flow area, or the effective propped fracture area is a consequence of proppant distribution within the fractures. Fracture permeability, on the other hand, is dependent on the size of proppant, concentration and sphericity of proppant being used.

Kern et al. 1959 conducted the first experimental work focused on describing the behavior of proppant transport within a fracture, and how various physical parameters contribute to the transport phenomena. Their investigation involved an experimental approach using a slot flow model to understand the dynamics of proppant transport within fracture system. They studied the transport of sand and water through two parallel plexiglass plates wherein sand initially settles to reach an equilibrium bed height and newly injected sand moves further into the slot. (Figure 1.2).

Another important study that followed this was conducted by Wang et al. 2009. The authors have proposed a three-zone proppant flow model based on the lab data from STIM-LAB and a power law correlation for the sand bed height in fractures with smooth surfaces. In the correlation, the bed height is a function of proppant settling velocity, fluid, and proppant Reynolds number. These studies were the earliest work on proppant transport in terms of experimental and empirical analysis. Since that time, many studies have been carried investigating other factors affecting proppant transport, both in crosslinked fluids and linear gels. The most recent studies have focused on low viscosity, slick water fracturing, most commonly in fracturing unconventional shales.

Industry still has incomplete knowledge in understanding slickwater fracturing in terms of proppant transport. Proppant behavior does not follow relationships developed from Stokes Law, used in crosslinked fluids. Hence, researchers have recently focused much attention on quantifying proppant transport behavior with slickwater.

Due to its low viscosity (1-10 cp) slickwater cannot carry proppant for a long distance, and cannot transport high concentrations. In slickwater fracturing, low concentrations (< 3 lb/gal) can be pumped at high rates (50-70 bbl/min) to create long fracture half-lengths. The high pump rates often lead to fracture completeness, meaning a network of secondary fractures develop and are connected to the primary, bi-wing fracture.

There are questions regarding how much sand enters these secondary fractures, as the fluid must turn flow directions to enter secondary fractures. This is an important consideration in evaluating SRV, because fractures that receive no proppant or very little proppant may end up closing and fail to contribute to well flow. Industry is divided in opinions regarding whether SRV is propped and contributes to flow (i.e. it is a good thing) or whether creating SRV simply wastes fracturing materials because these fractures remain unpropped (i.e. SRV is a bad thing).

There is a need to understand the distance to which the proppant can be transported within slickwater and factors affecting it. Previous studies in the literature have provided fundamental work, as presented in the literature review. These studies were carried out in two different approaches. One is the experimental approach where in the sub surface fractures are replicated at laboratory scale using fracture slots made of Plexi glass plates placed at desired widths. The other being the numerical modeling approach based on computational fluid dynamics using applications like Ansys FLUENT working in tandem with industrial fracture simulators.

Quantifying proppant transport is a challenging task as there are many treatment design variables that have an impact, in addition to formation and rock property variations, and stress regimes. Net pressure (the difference between bottomhole treating pressure and closure stress) is understood to affect induced fracture morphology, and then indirectly affect SRV. Hence, it is useful to consider those factors that are intrinsic in the net pressure calculation.

Ideally, fracture height, modulus, tip effects, viscosity and pump rate affect net pressure. Among these factors, pump rate and viscosity are the only two design parameters with very little effect on P_{net} (to the order $1/4$).

$$P_{Net} \propto \left\{ \frac{E'{}^4}{H_0^4} \left(\frac{Q\mu x_F}{E'} \right) + \frac{K_{Ic-App}{}^4}{H_0^2} \right\}^{1/4} \quad (1.1)$$

$$W \propto \frac{P_{Net}H}{E} \propto \left\{ \left(\frac{Q\mu x_F}{E'} \right) + \frac{H^2 K_{Ic-App}{}^4}{E^4} \right\}^{1/4} \quad (1.2)$$

In order to understand the proppant transport across different fracture geometries, attempts were made using Computational Fluid Dynamics applications and laboratory scale apparatus were created with bypass secondary fractures. Experimental models created were used for studying possible factors in the presence of secondary fractures. Factors like secondary fracture orientation, the existence of tertiary fracture were studied in recent times. The traditional approach for all the experimental models involved the continuous injection of proppant slurry using desired fracturing fluid until an equilibrium is reached on the settled dune heights in the fracture. This approach was very objective in

terms of understanding the proppant settling only after equilibrium is reached. Understanding the movement of proppant during the transition of proppant from settling phase to equilibrium phase is very important to know how the transport of proppant is occurring precisely. This study focusses on studying proppant transport meticulously with a systematic fracture pore volume injection approach, which can observe different stages of settling of proppant within the fracture. This however time taking from the previous approach provide much deeper insight in understanding the settling and transport of proppant within the fractures.

Also, as far as the study of complex fracture networks is concerned factors like heterogeneity of fracture width in presence of secondary slots, and different width of primary slot/secondary slot were limitedly studied. This study attempts to reduce the knowledge gap in terms of understanding fracture heterogeneity in complex fracture networks.

This study will be using equations developed by Alotaibi et al. 2015 to describe the distribution of proppant into the fracture systems. Alotaibi et al. 2015 stated that proppant settling in the fracture slots continues until the proppant bed reaches an equilibrium height. This height is called Equilibrium Dune Height (EDH). The ratio of EDH to the fracture slot height was termed as Equilibrium Dune Level (EDL)

$$\text{Equilibrium Dune Level (EDL), \%} = \frac{\text{Equilibrium Dune Height}}{\text{Fracture Slot height}} \times 100 \quad (1.3)$$

Proppant surface area fraction is defined as the ratio of surface area occupied by proppant within the fracture slot to the area of the fracture slot itself.

$$\text{Surface area fraction} = \frac{\text{Surface area occupied by proppant in fracture slot}}{\text{Fracture Slot surface area}} \times 100 \quad (1.4)$$

1.4. MOTIVATION

Proppant transport is a complex process, with numerous factors influencing the process of proppant transport. Although there have been studies conducted in this subject area, many historical studies are related to proppant transport with cross-linked, high viscosity fluids applied in conventional reservoirs. Studies regarding proppant transport in slickwater are in their infancy, and many factors have yet to be studied. The research of proppant transport in complex fracture systems is also in its infancy.

The historical literature does not comprehensively discuss the detailed stepwise process of proppant transport in the experimental studies. In addition, the settling mechanisms and correlations presented in previous literature are unique to the parameters specifically used in that study. Few studies address the effect of parameters like varying fracture widths on proppant transport. In addition, there is a need to examine varying fracture width along the primary slot in a complex fracture system. This work adds to, and extends the current slickwater proppant transport research work. An experimental apparatus is developed where varying input flow parameters will be used to account for different fracture widths and its effect on proppant distribution within completion fracture systems.

1.5. RESEARCH OBJECTIVES

The primary objective of this study is to provide a detailed insight on proppant transport within complex fracture slot using water as carrier fluid. Objectives of this study are as follows.

- Studying step wise development of proppant transport in slot flow apparatus by using fracture pore volume injection methodology
- Understanding the effect of flow rates, fracture width variation with a low-density ceramic proppant in a vertical planar fracture.
- Develop an experimental model with secondary fracture to understand the fracture complexity.
- Study of fracture complexity with a secondary slot apparatus and understanding the effect of width heterogeneity in complex fracture networks.

This study focuses on understanding how the transport of proppant occurs in fracturing systems with different flow parameters along a slot based vertical fracture model. The significance of the effect of proppant transport in a secondary fracture is significant focus of the work.

1.6. RESEARCH SCOPE

The scope of this study is presented in Figure 1.8. The experiments were conducted in two sets. The first set of experiments were conducted to investigate the effect of flow rate and fracture width in a primary fracture. The second set of experiments

were conducted to investigate the effect of varying the primary fracture width on proppant transport in primary and secondary fractures. Experiments were also conducted to study the effect of width heterogeneity in primary fracture on proppant transport.

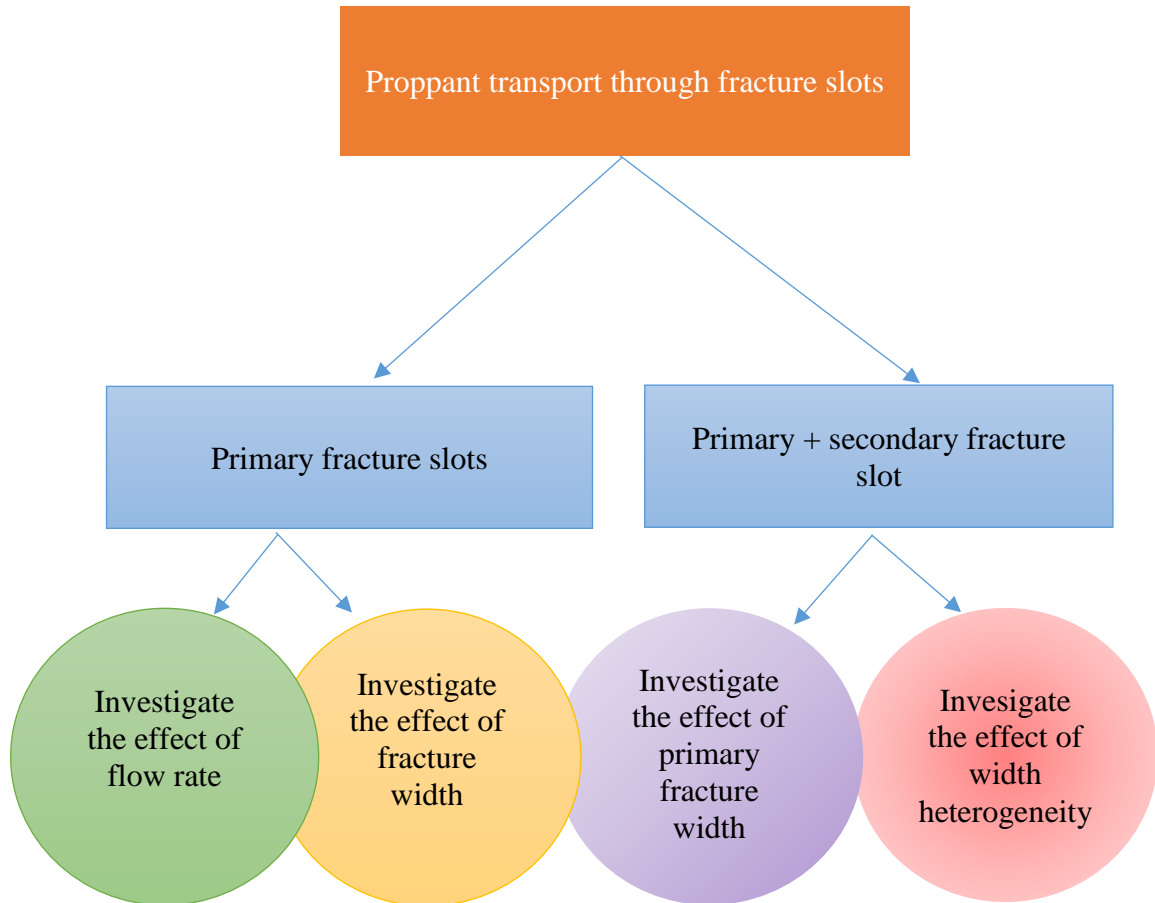


Figure 1.8. Research scope

2. LITERATURE REVIEW AND BACKGROUND

Proppant transport is an important case to be studied as it provides a deeper insight on propped fracture length which comprehends the results of hydraulic fracturing to stimulate well productivity (Kern et al. 1959). It is understood that there are multiple factors which influence the flow of proppant into the fractures. Several studies were conducted assuming specific factors related to the movement of proppant into the fractures. Kern et al. (1959) performed one of the earliest studies, wherein two Plexiglass were placed together at a certain width forming the fracture.

According to the study done by Kern et al. 1959, when the proppant is injected into the plexiglass setup the proppant deposits to the bottom of the fracture forming a dune shape structure. This dune continues to build up with the fracture till the fluid being injected reaches a certain critical velocity. Upon crossing this value, the fluid washes the already settled proppant further into the fracture till the velocity drops down to a critical value. Similarly, if the velocity is below the critical velocity, the proppant injected will settle until the critical velocity was attained again. Hence, critical velocity is also known as the equilibrium velocity.

Also, they stated the critical velocity was a function of the density difference between the fluid and proppant and is independent of carrying fluid viscosity. Measurement of equilibrium velocity was made by filling the fracture nearly full with sand and then flowing the fluid till no more of sand was washed out.

Kern et al. 1959 conclusions also stated that equilibrium velocity is higher for gelled fluids relative to Newtonian fluids. However, this study included the use of only one type of gelled fluid. The considerable difference in proppant transport properties was evident when using different types of liquids. Shah et al. 1982 developed a new approach for the setting of proppant when usage of Non-Newtonian Pseudoplastic fracturing fluids. His study develops Drag coefficient correlations as a function of fluid parameter n' . Earlier to this work was made by Harrington et al. 1981 developed similar correlations, however majority of these works were for static conditions along with some experiments with dynamic conditions.

Based on the above initial studies it was evident that the fracturing fluid rheology defines proppant transport in hydraulic fractures to a major extent. Hence as we go further into this section it is easy to classify the study done in proppant transport into two major categories based on carrier fluid followed by literature discussing the factors that influence proppant transport

- PROPPANT TRANSPORT IN CROSSLINKED FLUIDS
- PROPPANT TRANSPORT IN SLICKWATER FLUIDS
- FACTORS INFLUENCING PROPPANT TRANSPORT

2.1. PROPPANT TRANSPORT IN CROSSLINKED FLUIDS

Studies made initially were predominantly based on fluids, which were more viscous, and crosslinked fluids. Initially, there were studies from Visser et al.1974

wherein the build up of proppant dune was studied. Their work focused on measuring equilibrium velocity and sets of equations were presented that could be used to predict proppant bed heights and lengths. This was followed by a study in settling of single particles under shear in concentric cylinder devices by Novotny et al. 1977. An interesting conclusion made in his study is that proppant settling during the fracture closure time plays a major role in the distribution of proppant in the fracture. His work also defines the importance of non-Newtonian characteristics, wall-effect and concentration effect and shear rate effect on proppant settling.

This was followed by vertical slot flow model work done by Clark et al. 1981. These studies stated that settling in shear and stagnant fluids deviate from Stokes law settling. Gruesbeck et al 1982 performed an experimental and theoretical studies of particles transported through perforations during fracturing operations. They indicated the in order to avoid the bridging of particles at perforations the particle diameter should be 6:1 or larger. They indicated the particle movement is under the influence of gravity and inertial forces. Roodhart et al 1985 in his paper provided an explanation for this behavior by introducing the term “anisotropic apparent viscosity”. However, anisotropy in viscosity only becomes important at shear rates of 25 s^{-1} where as the fluids used in fracturing treatments experience a shear rate less than this value. Understanding the shear rates at which the fracturing treatment occurs was important as it determines the proppant carrying capacity. To understand the importance of shear rates, Clark et al. 1985 in their study on proppant transport by Xanthan and xanthan-hydroxy propyl guar discusses how fracturing fluids such as HPG solutions and Xanthan behave at different shear rates. He

justifies in his paper that fluid properties measured at low shear rates are a better indicator of proppant transport than standard test shear rates as they are reflective of fracturing environment. It was evident that settling velocity in steady flow could be understood using Stokes law, however settling velocities in unsteady flow and flow in cross-linked fluids deviate from stokes law calculations. Early in to the 2000's most of the research was focused to study of proppant transport in slickwater systems. This will be discussed in Section 2.2.

2.2. PROPPANT TRANSPORT IN NON-VISCOUS FLUIDS

The use of conventional crosslinked fluids in low permeability reservoirs was relatively less to that of slickwater. Use of these less viscosity fluids allow the creation of long narrow fractures in the reservoir without major height growth. However, due to the low viscous nature proppant transport in Newtonians fluids has its own challenges in terms of settling equations. Stokes settling model alone does not seem to be adequate as it is limited to static settling of particles at low Reynolds number.

Proppant transport equations were improved with frequent improvisations in settling velocity equations were made. Table 2.1 summarizes recent studies dealing with proppant transport in water fracs and slickwater proppant transport. The table provides a brief description of each study followed by the type of fracture fluid and proppant used in each study.

Table 2.1. Recent literature on slickwater fracturing (experimental and CFD)

Literature (Year)	Fracture Fluid	Proppant Used	Breif description of the work
Ngameni et al. 2017	Water	100 Mesh, 40/70 mesh, 20/40 Mesh	Proppant distribution among perforation clusters in horizontal wellbore
Dhurgham et al. 2017	Distilled water	40/70 Ceramic (LWC)	Experimental Study of heterogenous fracture width, wall roughness and leak-off using slot flow model. Proppant settling mechanisms.
McAndrew et al. 2017	Foam Based fluid (N ₂ base)		CFD and experimental modelling of proppant transport in foam based fluid
Tong et al. 2016	Water	20/40, 40/70 Sand	Study of Fracture complexity. Proppant transport in slot flow model with varying orientation of secondary fractures.
Li et al.2016	Slickwater	40/70, 30/50 Sand	Experimental modelling to study the effect of sand ratio, particle size, angle of secondary fracture.
Chang et al. 2016	Slickwater	40/70, 20/40	Developed proppant transport model (CFD) and parametric study on effect of fracture fluid viscosity, effect of natural factors, and effect of difference in horizontal stresses
Alotaibi et al. 2015	Slickwater	30/70 Sand	Settling mechanism of sand with slickwater as carrier fluid. Defined equilibrium dune level. Studied the movement of proppant into secondary fractures.
Blyton et al. 2015	Slickwater/high concentration gels	40/60, 20/400, 16/30	CFD –DEM simulations to study the effect of fluid rheology, proppant density, Reynolds number on settling velocities.
Mack et al. 2014	Slickwater	60/70, 50/60, 40/50, 30/40 Ceramic.20/40 Intermediate strength Ceramic	Experimental study to measure the material properties governing saltation and repetition (settling mechanisms). Used advance ceramic proppant.
Sahai et al. 2014	Slickwater	20/40, 30/70,100 mesh natural sand	Study of effect of complexity, pump rates and proppant size on proppant transport
Kostenuk, N. H. et al 2010	Slickwater	40/70 Sand PTM – proppant transport modifier	New proppant transport method by modifying the surface property of proppant which reduces settling
Palisch et al.2008	Slickwater	20/40, 30/50 and 40/70 Sand and Resin coated sand.	Benefits and advantages of slickwater fracturing. Discusses the inability of stokes law to predict true transport of proppant in slickwater treatments.
Gadde et al.2004	Water		Developed correlations to allow fracture models to account for inertial effects, proppant concentration, fracture width and turbulence on settling

As an initial attempt, Gadde et.al. 2004 in their study, developed proppant settling model where the effect of fracture walls, rheology, proppant size, fracture widths are taken into consideration. Studies discussed in Table 2.1 were focused on proppant settling in water fractures wherein less viscous fluids are used (slickwater). Figure 2.1 and Figure 2.2 depict the effect of diameter of proppant on settling rate and particle Reynolds number from the correlations developed. They also show the deviation of predicted settling velocities from stokes settling velocities.

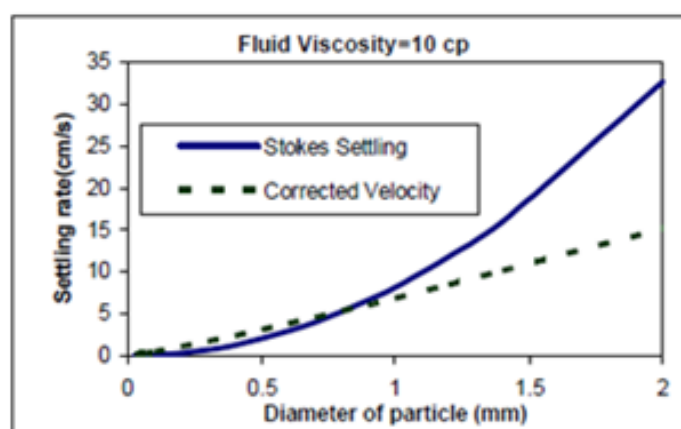


Figure 2.1. Settling velocity corrected to inertial effects

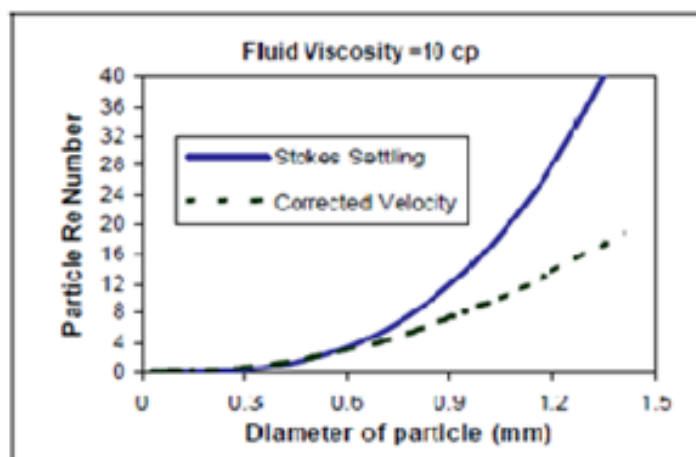


Figure 2.2. Particle Reynolds number as a function of radius

Gadde et al. 2004 work indicates that Stokes settling velocity is valid for small particles ($Re_p < 2$) in the absence of wall effects. However, in the case of large particle Reynolds number the settling velocity is given by multiple correlations. These correlations have been presented as one single where settling velocity is presented as a function of particle Reynolds number.

Similarly, relations for effect of proppant concentration, fracture width, turbulence on settling velocities were presented in the study done by Gadde et al 2004. Later, the correlations were incorporated as one single dynamic model into custom developed the frac simulator. The results from the simulator provided a deeper insight into the importance of considering settling correlations when modeling proppant transport. However, the experimental verification has not been provided on these factors. We will discuss in brief regarding the factors influencing slickwater proppant transport in the below Section 2.3.

2.3. FACTORS INFLUENCING PROPPANT TRANSPORT

As mentioned in previous Section, there are multiple factors which influence the proppant transport in different possible ways. Important among them are fracture fluid properties, fracture geometry, and complexity. Slot flow experiments (Bacchcock et al. 1967; Kern et al. 1959; Medlin et al. 1985; Clark et al. 1989; Patankar et al. 2002; Wang et al. 2003, Woodworth and Miskimins 2007) were conducted previously to understand these factors in vertical fracture slots. This was followed by a series of studies (Sahai et al. 2014; Alotaibi et al. 2015; Li et al. 2016; Tong et al. 2016; Chang et al.; 2016;

Dhurgham et al. 2017) in order to understand the effect of complexity. A brief overview of the results will be provided in this Section.

2.3.1. Fluid Flow Properties. Fluid flow properties have a major impact on transport of proppant into the fracture. Explanation of this effect can be explained best by work done by Clark et al. 1989. He described in brief the forces acting on the slurry while moving into the fracture slot. The first is the horizontal force that pushes the slurry down along the length of the slot and second is the horizontal force acting to pull the slurry to the bottom of the fracture. While horizontal force depends on flow rate and fluid properties, the gravitational force depends on the density difference between the fluids. He defined a dimensionless group called as Dimensionless convection number (equation 2.1 and 2.2) to understand the behavior of both Newtonian and power law fluids. His experiments were based on this dimensionless group where in a value of $Nc > 1$ implied higher horizontal forces and greater transport of proppant into the fracture is possible. Similarly $Nc < 1$ implies more settling of proppant due to gravity. Figure 2.3. shows a proppant particle entering a fracture slot and forces acting it as mentioned above.

$$Nc = \frac{F_H}{F_v} = \frac{12q\mu}{gw^3\Delta\rho} \quad (2.1)$$

$$Nc = \frac{F_H}{F_v} = 2 \left(4 + \frac{2}{n}\right)^n \frac{12qq^n}{gw^{2n+1}\Delta\rho} \quad (2.2)$$

In the Equations 2.1 and 2.2, q is the injection rate divided by the height
 μ is the viscosity of injection fluid
 $\Delta\rho$ density difference between injected fluid and fluid in slot
 W is the slot width, and n & k are the power law parameters.

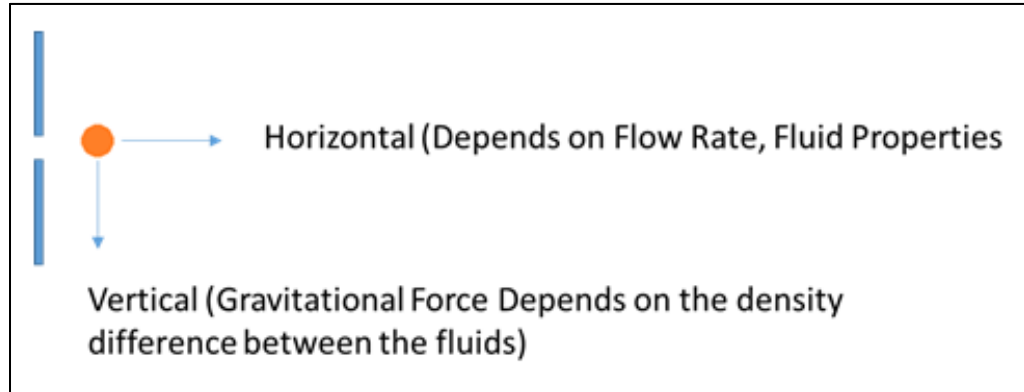


Figure 2.3. Force acting on a proppant particle entering a fracture slot

Particle settling velocities are important parameters, which primarily depend on fluid properties and fluid flow. Initially, single particle settling in Newtonian fluids are well defined by creeping flow regime of Stoke's law or modified Stokes law. (Equations 2.3, 2.4 and 2.5)

$$v_s = \frac{g(\rho_p - \rho)d^2}{18\mu} \quad (2.3)$$

$$v_s = 0.2 \left(\frac{g(\rho_p - \rho)d^2}{18\mu} \right)^{0.72} \frac{d^{0.72}}{(\mu/\rho)^{0.45}} \quad \text{for } 1 < N_{Re,p} < 1000 \quad (2.4)$$

$$v_s = 0.2 \left(\frac{g(\rho_p - \rho)d^2}{\rho} \right)^{0.5} d^{0.5} \quad \text{for } N_{Re,p} > 1000 \quad (2.5)$$

Based on the above relations defined by Stokes law for different Reynolds number density difference between the proppant particles are key parameters defining the settling velocities. There are several other correlations developed to understand the settling velocities for different flow regimes (for different Reynolds number) as turbulence affects particle settling and proppant transport. We will not be discussing in detail regarding these correlations as settling velocity is not an integral part of this study. However, we can interpret the results obtained to reiterate and verify the previous literature.

2.3.1.1. Effect of pump flow rates. Similar to the study made by Clark et al.1989 in slot flow the force acting on immersed particle is orthogonal to the flow. The lift force is as a result of particle rotation, shear, and inertia in the fluid. Effect of horizontal flow is believed to decrease the particle settling rate. In hydraulic fracturing treatments, especially in water fracs, the horizontal flow rate is high resulting in turbulent flow in fractures. The effect of turbulence is supposed to increase the settling however, laboratory tests conducted by Liu et al, 2006 have shown that such effects (which includes turbulence and lift) are small under normal hydraulic fracturing conditions.

A number of studies followed to understand the effect of flow rates on proppant transport. Kern et al 1959 in their preliminary studies showed that bed of settled sand builds up in the bottom of the vertical fracture unless injection rate per foot of formation is very high. Sahai et al. 2014, in his study of laboratory scale experiments, showed that pump rates directly affect the proppant transport and settling in fracture slots. He defined

a term called threshold pump rate which is the pump rate of which the proppant moved in to fracture networks i.e. the secondary fracture slots. However, an interesting conclusion from his study was that effect of proppant transport was found to be different in primary and secondary fractures that will be explained in detail in the Section discussing the effect of fracture complexity.

Alotaibi et al. 2015 showed that EDL follows a nonlinear relationship (power law trend) with increasing slurry velocity. The study showed the EDL decreases with an increase in slurry velocity.

2.3.2. Proppant Properties. Proppant properties in fracture treatments have a high degree of influence in proppant's transport ability into the fractures. As mentioned in earlier Sections, proppant density relative to carrier fluid density highly influences the settling of proppant in the fractures. Higher the density, the faster it settles reducing the distance of travel for the proppant. Proppant properties ranging from proppant type, proppant size, proppant grain shape have their individual effect on proppant transport. We will discuss in detail regarding effect of these proppant properties on the transport ability.

2.3.2.1. Effect of proppant size on proppant transport. Palisch et al. 2008 mentioned in his study that as particle diameter increase, the settling velocity of that particle increases. The size of the particle has an exponential relationship to settling velocity. In slickwater fracturing, it is intuitive to assume that proppant density is the

primary driver for proppant transport. However, while proppant density is certainly important, the size of proppant particle actually has a larger effect of proppant settling than density. Proppant size bears an important relationship with settling of proppant.

Palisch et al. 2008 provides a simple illustration to explain the effect of proppant size. It is common that many in the industry would not consider pumping in denser proppant like bauxite in slickwater fracturing. However, the fact is that the settling rate of 20/40 sand is actually 50% greater than 40/70 bauxite. This makes it obvious that the 40/70 sand/RCS and 40/80 LWC are widely used in industry (Refer Figure 2.4). It is noteworthy, that all of the above-mentioned proppants i.e. 20/40 sand, 40/70 bauxite, 40/70 Sand/RCS and 40/80 LWC settle at a lower rate than 20/40 sized 1.75 ASG "ultra lightweight" proppant. This does not rule out the usage of ultra weight proppants, however, consideration to proppant size is necessary along with proppant density while understanding proppant transport.

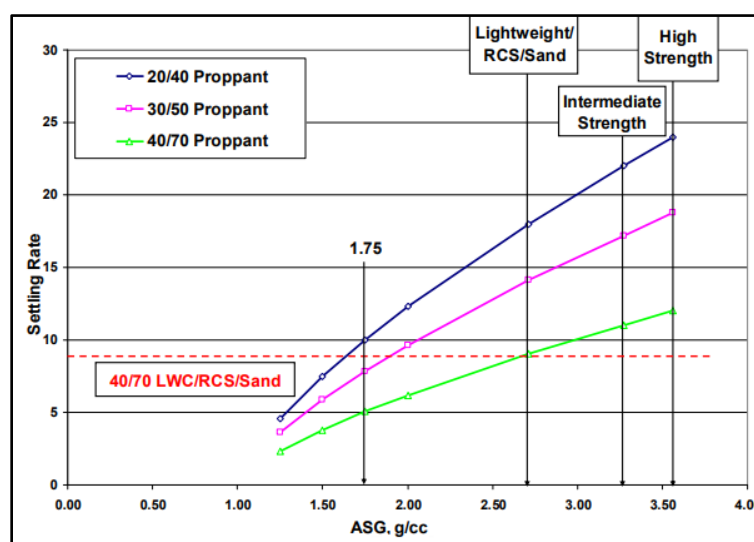


Figure 2.4. Settling rate for various proppant sizes

Sahai et al. 2014 as a part of his study conducted laboratory experiments to understand the effect of proppant sizes. With the usage of proppant of different sizes, he conducted the slot flow experiments for 100 mesh sand, 30/70 mesh sand. It was observed that most of bigger particles were deposited within the slot while lighter particle sizes transported out of the slot.

Another interesting observation made in the study by Sahai et al. 2014 was that there was higher segregation of sand particles at higher pump rates. The primary consequence of Proppant sizes is directly proppant conductivity in fracture more than proppant transport. Fracture post fracture conductivity is responsible for the production rise.

2.3.2.2. Effect of proppant concentration. Several correlations were developed to understand proppant concentration affect on proppant transport in fractures. Correlations were based on settling velocity, which will, in turn, helps in understanding proppant transport. Gadde et al. 2004 summarized each of these correlations in the Figure 2.5, which helps in determining the settling velocities for different concentrations. The graph shows high concentrations tend to decrease the particle settling velocity

Liu et al. 2005 studied the effect of particle concentration using slot flow model where he states that in regions of higher proppant concentration particles move at significantly slower velocity than particles at low concentration.

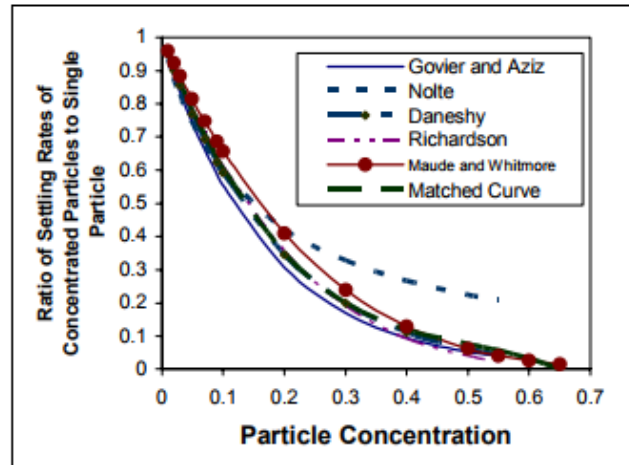


Figure 2.5. Correlations proposed to understand the effect of concentration on settling velocities (Gadde et al, 2004)

Dayan et al. 2009 stated decrease in settling velocity with concentration occurs due to change in the fluid flow around the volume fraction of particles and is referred to as hindered settling by Sahai et al. 2014 based on the laboratory results concluded the higher proppant concentrations resulted in lower proppant dune heights. Although more proppant is being pumped into the fracture slot the resultant dune height is lesser relative to that at a lower concentration. However, Alotaibi et al, 2015 also studied the effect of concentration on proppant transport showing the Equilibrium dune level increases with increase in concentration. He attributed the EDL increase to an increase in the wall-to-wall interactions with an increase in concentration.

2.3.3. Effect of Fracture Complexity. In order to understand the effect of complexity series of studies were conducted starting Sahai et al. 2014; Alotaibi et al. 2015; Li et al. 2016; Tong et al. 2016; Chang et al.; 2016. Most of these studies were based on slot flow experiments along with numerical modeling using CFD simulations.

Sahai et al. 2014, showed that efficiency with which the proppant travels across secondary fractures is dependent on the combined effect of slurry rate, proppant concentration, and proppant size. Based on the results from this study, relative position of the secondary also resulted in different proppant due to turbulent flow at the top of the slot

Alotaibi et al. 2015 on the other hand study showed that fracture network complexity is not a major limiting factor for slickwater proppant transport as long as enough proppant is injected to develop the dune heights in fracture slots. EDL heights of 96% were achieved in secondary and tertiary fractures in his study.

Tong et al. 2016 extended Alotaibi et al. 2015 work by conducting experiments with secondary fracture slot oriented at different angles to primary slots. He conducted experiments at three different angles i.e. 45°, 90° and 135° degrees. Maintaining constant proppant size and shear rate, it was seen that sand bed length in the secondary slot is largest in 45° cases and smallest in 135° case. Sand bed shapes in main slots remained similar. CFD Simulations were also performed in this study. Li et al. 2016 worked on understanding the change in proppant transport for a change in orientation of secondary slot (30°, 60° and 90°). Unlike results stated earlier, there was a decrease of dune height in the primary fracture for an increasing orientation angle of the secondary slot. Dune height also decreased in secondary slots with an increase in orientation angle of the secondary slot. Dhurgham et al. 2017 studied the effect of heterogenous fracture width in primary fractures. Their study also included the investigation of proppant settling

mechanisms in the presence of factors such as heterogenous fracture width, fracture roughness and leakoff. Dhurgham et al.2017 work showed that proppant bed heights increased with heterogeneity along a single primary fracture.

However, study by Dhurgham et al. 2017 could not capture the effect of varying width in presence of secondary fractures. In reality, the flow during fracturing is more complex and needs the understanding of the variation of width in fractures. This study attempts to understand the effect in which there is no constant width of primary and secondary fractures.

3. EXPERIMENTAL DESCRIPTION AND PROCEDURE

3.1. EXPERIMENTAL APPARATUS

The experimental apparatus was developed to understand proppant transport for complex fracture systems. The experiments were based on injection of proppant into a plexiglass apparatus, which is two parallel plexiglass sheets placed together. These sheets are made of acrylic and have a smooth surface on sides. (See Figure 3.2). The apparatus was majorly used in two different configurations based on the factors to be studied in regards to proppant transport.

Figure 3.1 illustrates the two configurations mentioned below.

- (1) Primary fracture
- (2) Primary and Secondary fracture

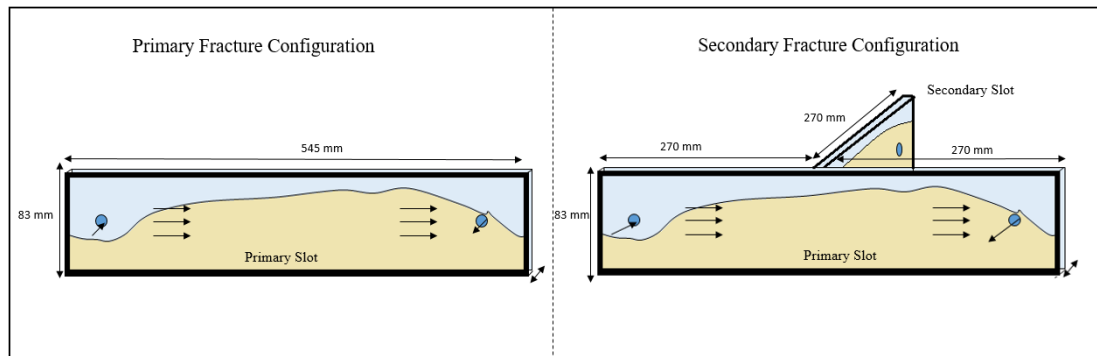


Figure 3.1. Comparison of primary and secondary configurations of the apparatus

3.1.1. Primary Fracture. This configuration of apparatus has only the primary wing of the fracture (Figure 3.2) The parallel plate setup consists of a neoprene rubber sheet to create the width for the fracture slot in which proppant movement is analysed. The slot width was adjusted using a neoprene rubber sheet placed in between the

plexiglass plates. The height of slot was 83 mm and length was 535 mm as shown in Figure 3.2.

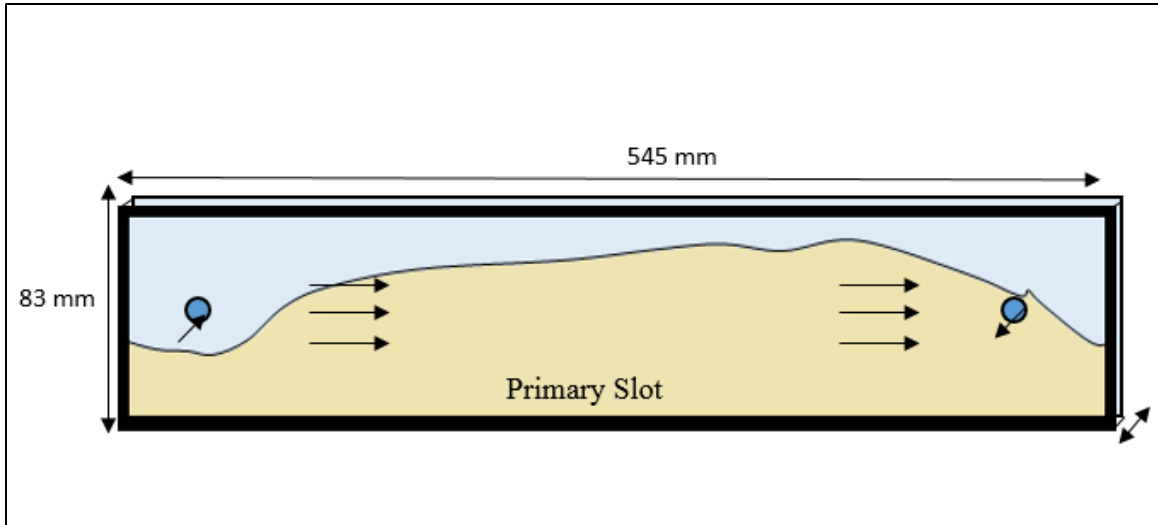


Figure 3.2. Plexi glass setup for primary configurations of the apparatus

The inlet and outlet diameters were 4 mm each placed half way across the height and 50 mm from edges of the slot. A proppant collecting jar was placed along the outlet to collect the proppant flowing out of the apparatus.

The apparatus includes an accumulator, which is a cylindrical container where proppant and water were mixed in desired proportions before injecting into the primary fracture (Figure 3.3) The accumulator has an inlet for nitrogen on the side of cylinder placed an inch of the bottom. It has an outlet at the bottom of the accumulator to allow the flow of proppant slurry. The nitrogen was injected from Nitrogen source tank, which holds pressurized nitrogen. Pressurised nitrogen was primary driving source for the slurry

to move into primary slot. Injection pressure of nitrogen was used to maintain the desired flow rates.

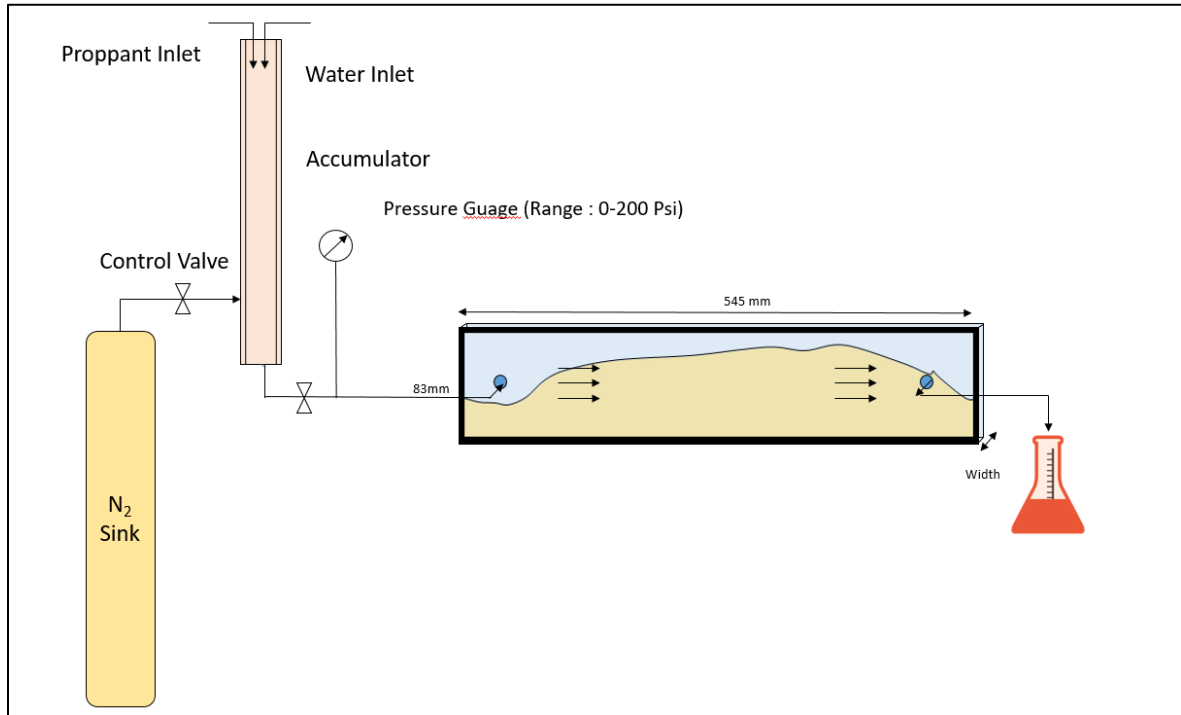


Figure 3.3. Experimental setup with the parallel plate apparatus

Inlet pressure for the slurry moving into the slot was measured using a pressure sensor and data logging kit. Pressure sensor was calibrated after every experiment to maintain precision and accuracy. The studies done with primary wing establishes the behavior of proppant traveling in a single direction without any deviation. In order to verify the flow behavior of proppant that is mentioned in the previous studies, few initial experiments were conducted. Primary fracture configuration was primarily used to understand the effect of flow rates and fracture width on proppant transport. Different widths were used with this configuration, it is important to note that the width of primary

fracture remained constant in these experiments. Figure 3.3 illustrates the primary configuration of the apparatus.

3.1.2. Primary and Secondary Fracture. This configuration of the apparatus was used to study the effect of complexity on proppant transport. It was developed by building a secondary slot with two plexi glass sheets half the length of the primary slot and with same height of 83mm. The width of slot is dependent on the neoprene rubber sheet as explained above. This configuration of apparatus had an outlet at the end of secondary slot. Building the apparatus with secondary slot right across the half way has one basic advantage. The distance to which the proppant transport occurs past the half way mark in primary slot remains equal in primary slot and secondary slot. This gives a better understanding in terms of proppant transport for various widths.

The flow of slurry in this configuration is not unidirectional because of presence of secondary slot. The flow diverts half way into the primary distributing itself into two streams. Part of the slurry continues through the primary slot and the other turns around 90° to flow into the secondary slot.

Figure 3.4 shows the apparatus built for this study with both primary and secondary fracture. Figure 3.5 and Figure 3.6 illustrate the plexi glass setup and schematic of apparatus with primary and secondary fractures.

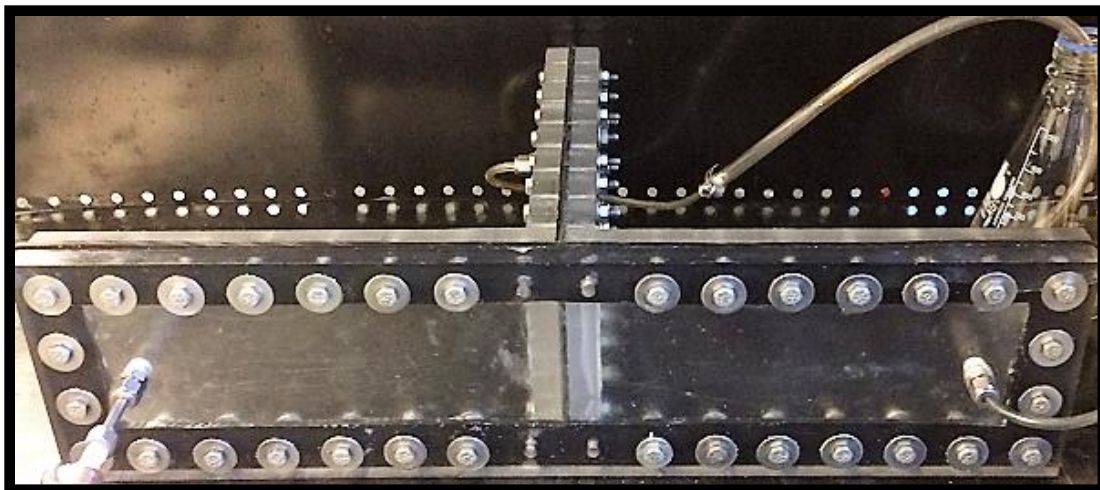


Figure 3.4. Secondary fracture apparatus setup

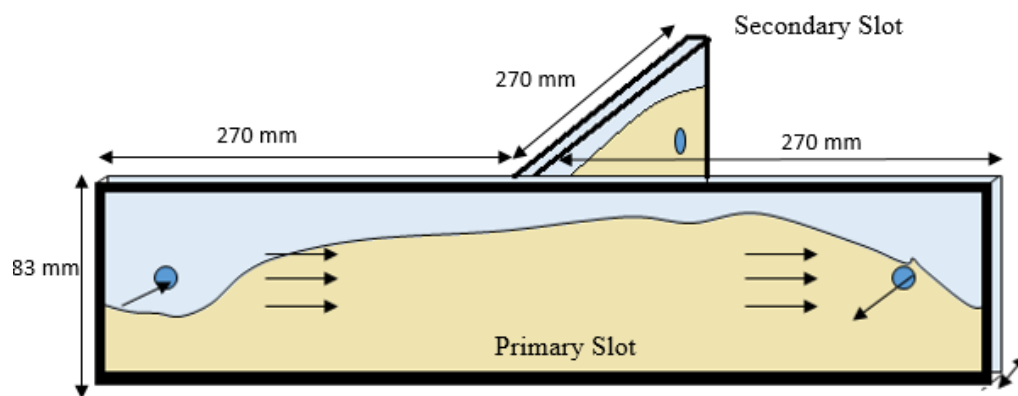


Figure 3.5. Plexi glass setup for apparatus with primary and secondary fractures

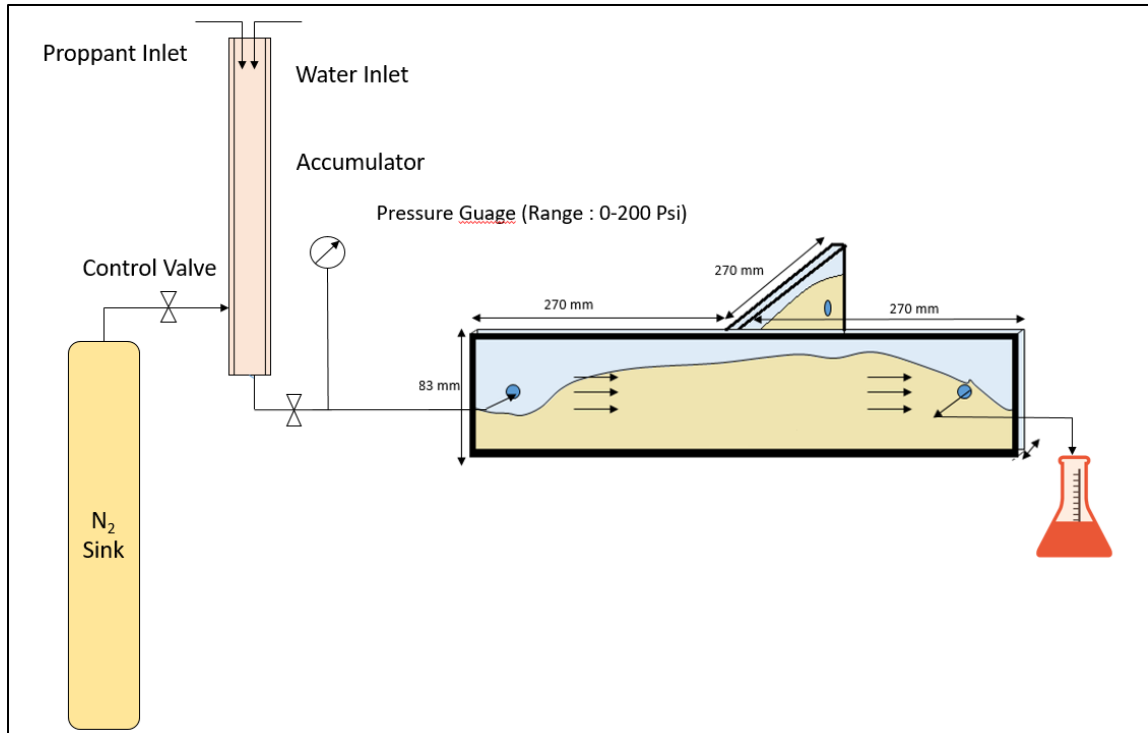


Figure 3.6. Schematic with primary and secondary fractures

The objective of the experiments using secondary apparatus understands the effect of the change in width in complex fracture networks. Three different experiments were conducted in this study. Three of these cases are illustrated in Figure 3.7

Case 1: The primary fracture width and secondary fracture width to be constant.

Case 2: The primary fracture width is greater than the secondary fracture width.

Case 3: The primary slot had a width variation half way along the slot length.

Width heterogeneity ratio $W_{in}/W_{out} = 2$.

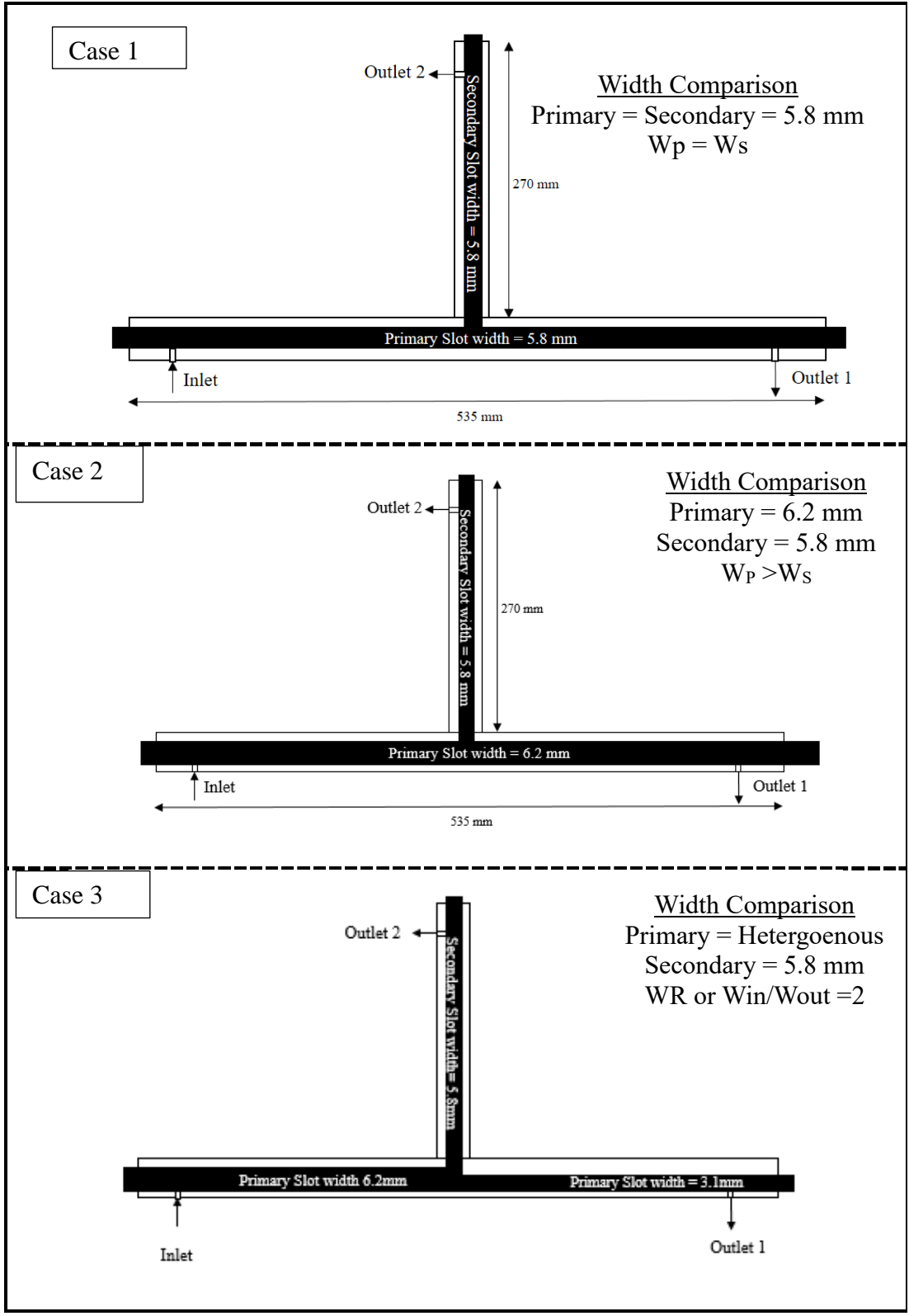


Figure 3.7. 3 different cases for experiments in primary and secondary fractures

3.2. EXPERIMENTAL DESCRIPTION

The effects of injection flow rates and fracture widths were studied initially at a constant concentration of slurry. The proppant flow was captured using a camera placed perpendicular parallel plate apparatus. The concentration of slurry is maintained around 1.67 lb/gal which is typical field proppant concentrations for Slickwater proppant transport. The width of fractures were altered to maintain required fracture width to proppant diameter ratios (W/D).

The experiments were carried out based on the different controlling parameters of proppant transport. Flow rate, fracture width and complexity are three major parameters of investigation in this study. Table 3.1 summarises the experimental parameters that were used while studying the effect of flow rates on proppant transport. Fracture width and concentration of proppant slurry were maintained constant during this set of experiments.

Table 3.1. Parameters used to study the effect of flow rates on proppant transport

Proppant Experiments used to study the effect of flow rates				
(Number of Experiments : 3)				
Flow Rates(GPM)	Concentration (lb/gal)	Slurry Velocities (mm/sec)	Fracture width	Injection pressure (Psi)
0.14	1.67	18.3	0.228 in	5
0.3	1.67	39.3	0.228 in	30
0.4	1.67	52.4	0.228 in	50

Table 3.2 summarises the details of experimental parameters that were used to understand while studying the effect of fracture width on proppant transport. Fracture widths were varied from 0.5 mm to 9.5 mm (for fracture width to proppant diameter ratio of 1.18 to 22.8). This makes sure that the effect of proppant transport for proppant diameters comparable to fracture width are studied comprehensively.

Table 3.2. Parameters to study the effect of fracture widths on proppant transport

Proppant Experiments used to study the effect of fracture width				
(Number of experiments: 6)				
Flow Rates(GPM)	Concentration (lb/gal)	Slurry Velocities (mm/sec)	Fracture width	Injection pressure (Psi)
0.4	1.67	52.4	0.377 inches	50
0.4	1.67	52.4	0.228 inches	50
0.4	1.67	52.4	0.122 inches	50
0.4	1.67	52.4	0.0551 inches	50
0.4	1.67	52.4	0.0378 inches	50
0.4	1.67	52.4	0.0196 inches	50

Table 3.3 summarises the parameters used to study the effect of varying primary fracture width in setup with primary and secondary fracture setup. Fracture width of secondary fracture is maintained constant along with the parameters like flow rate and concentration. This Table includes the parameters used to study the heterogeneity in fracture networks.

Table 3.3. Parameters used to study the effect of fracture complexity

Proppant experiments used to study the effect of fracture width in secondary fractures					
(Number of experiments: 6)					
			Fracture width		
			Primary	Secondary	
0.4	1.67	52.4	5.8mm	5.8 mm	50
0.4	1.67	52.4	6.2 mm	5.8mm	50
0.4	1.67	52.4	6.2 mm	3.1 mm	50

3.3. EXPERIMENTAL PROCEDURE

- Proppant and distilled water were mixed in a cylindrical accumulator to get a required concentration of proppant before injection.
- Pressure sensor was calibrated to atmospheric pressure
- A control valve regulated the flow of proppant slurry from the accumulator into the parallel plate apparatus. The other control valve at the side of the accumulator controlled the flow of pressurized nitrogen. Nitrogen pressure is set to desired value
- Nitrogen travels through the hose from nitrogen source tank to the accumulator pushing the slurry in accumulator into the fracture apparatus.
- The pressure sensor installed at the inlet of plexiglass measures the inlet pressure of proppant slurry. Pressure from nitrogen tank pushes the slurries into the apparatus at required flow rates.

- Each injection into the fracture slot apparatus results in some volume of the proppant settling in the fractures and some volume of proppant travelling through the outlet .
- The slurry as it enters the parallel plate apparatus settles and travels under the influence of various factors like flow rates, viscosity, and other fluid parameters.
- The settling occurs and height of sand bed increases continuously. The settling continues until a certain height is reached where no further settling takes place. At equilibrium bed height, there is no further increase in proppant bed height is seen.
- These heights are measured at multiple points from the inlet to the end of parallel plate apparatus as shown in Figure 3.8.
- Heights and lengths to which proppant travels were measured at different points along the fracture slot manually and using image digitizing technique. The proppant that travels out of the outlet was collected in a measuring jar.
- The pressure sensor installed near the inlet also indicates the flow period of slurry where a pressure peak seen during the proppant's injection into parallel plate apparatus. The time difference is used to measure accurate flow rates.
- The proppant slurry as mentioned was injected in multiple stages in order to observe the settling pattern in the fracture slot until proppant bed reaches the equilibrium height.
- Every injection of proppant will be considered an injection of one fracture pore volume (FPV) of slurry.
- The proppant settles at various points along the fracture as the dune builds up and the same concentrations and flow rates were used until the proppant bed height

reached an equilibrium. The number of fracture pore volumes injected are counted till equilibrium is reached.

- Equilibrium dune level and proppant surface area fractions are measured for each experiment

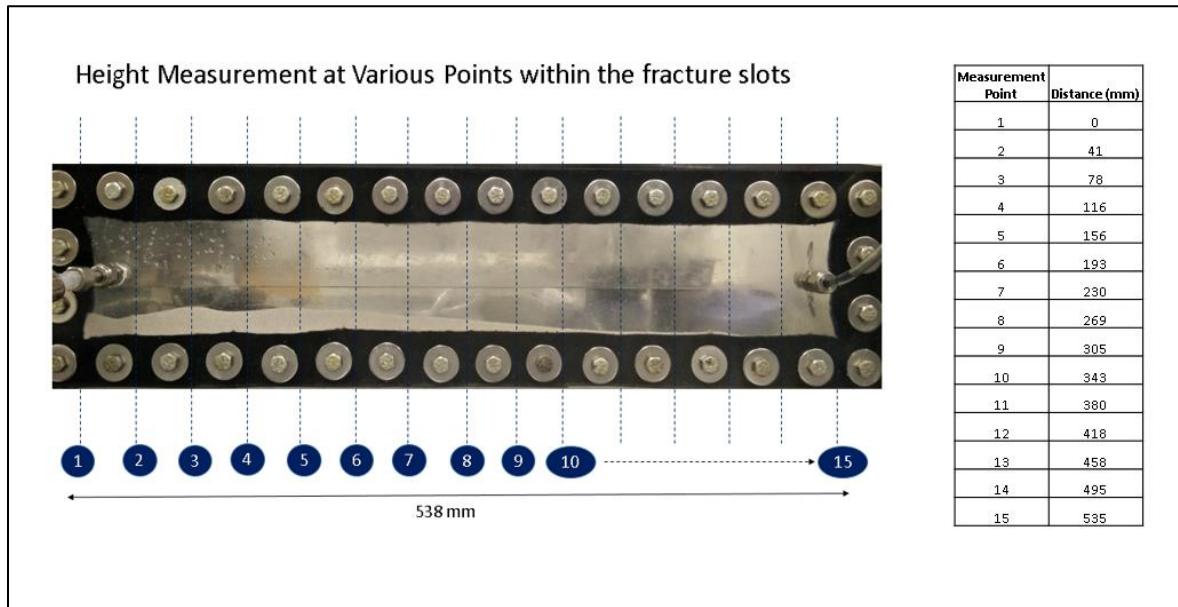


Figure 3.8. Measurement of heights at various points within fracture slots

4. RESULTS AND ANALYSIS

Experimental results in this study provided a significant understanding of the proppant transport and settling in fracture networks under the influence of parameters such as flow rates, frac width to proppant diameter (W/D) ratios etc. Each of these factors has a significant influence movement of proppant across the plane along the fracture slot (both vertically and horizontally).

Experimental results in this study will be presented in two parts that are results for Primary Fracture apparatus will be presented which includes understanding the effect of flow rates, inertial forces and fracture widths. This will be followed by results for Secondary Fracture apparatus where individual widths of primary and secondary fracture are the varied and consequent effect of proppant transport is studied.

4.1. RESULTS FOR PRIMARY FRACTURES

The below Section 4.1.1 includes the effect of the flow rate/slurry velocity, fracture width, and size of proppant relative to the width of the fracture slot. Results will include the measured height and length of proppant beds settled in the fracture slots. Comparison of bed height at equilibrium (equilibrium dune levels), the surface area covered by the proppant will be discussed to quantify the effect of each parameter.

4.1.1. Effect of Flow Rate on Proppant Transport. The behavior of proppant transport at various flow rates show a significant difference in the settling behavior with a change of flow rates. Due to the low viscosity of water, proppant initially settles near to

inlet and as the proppant dune builds up some of the proppant is pushed further towards the outlet. Higher flow rates resulted in higher slurry velocities within the parallel plates.

In this study, three different flow rates were used. 0.14 GPM, 0.3 GPM, and 0.4 GPM. The concentration of 1.67 lb/gal is used to replicate the field slickwater concentrations. Effect of flow rate on proppant transport can be quantified based on variables proppant bed height, distance to which the proppant has traveled and a number of injections to reach equilibrium.

Figure 4.1. depicts the settling of proppant bed in fracture slots for injection of each FPV. The figure shows a continuous increase in proppant bed height for each fracture pore volume injection until proppant bed height reaches a equilibrium. This can be noticed with overlapping curves in Figure 4.1. there is no change in proppant bed height post equilibrium is reached.

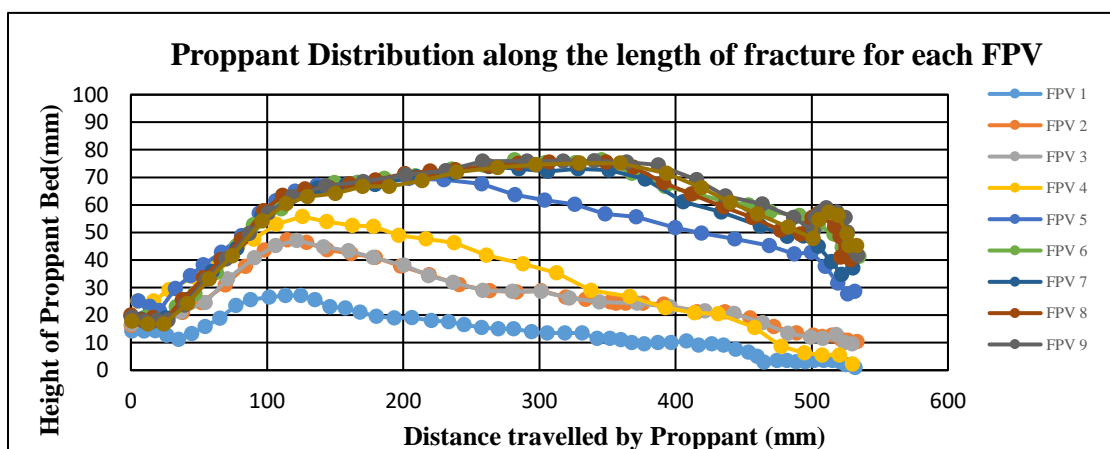


Figure 4.1. Development of sand dune heights as it reaches equilibrium

In order to understand the effect of injection flow rates on proppant bed height we compare the distribution pattern for each flow for all the flow rates tested in this study. A major difference can be seen in distribution pattern at end of FPV 1 followed by proppant distribution pattern at equilibrium. From the Figure 4.2. Proppant distribution at end of FPV 1 for different flow rates it is evident, that the proppant slurry in the case of lowest flow rate i.e. 0.14 GPM settles more towards the inlet and concentrated in a first half wing of the fracture slot. This is due to very less horizontal force available to transport the proppant deeper into the fracture. For the highest of flow rates, i.e. 0.4 GPM the proppant transports much deeper into the fracture. Higher flow rates subject the proppant to a greater horizontal force. This imparts a greater transport ability of proppant into the fracture.

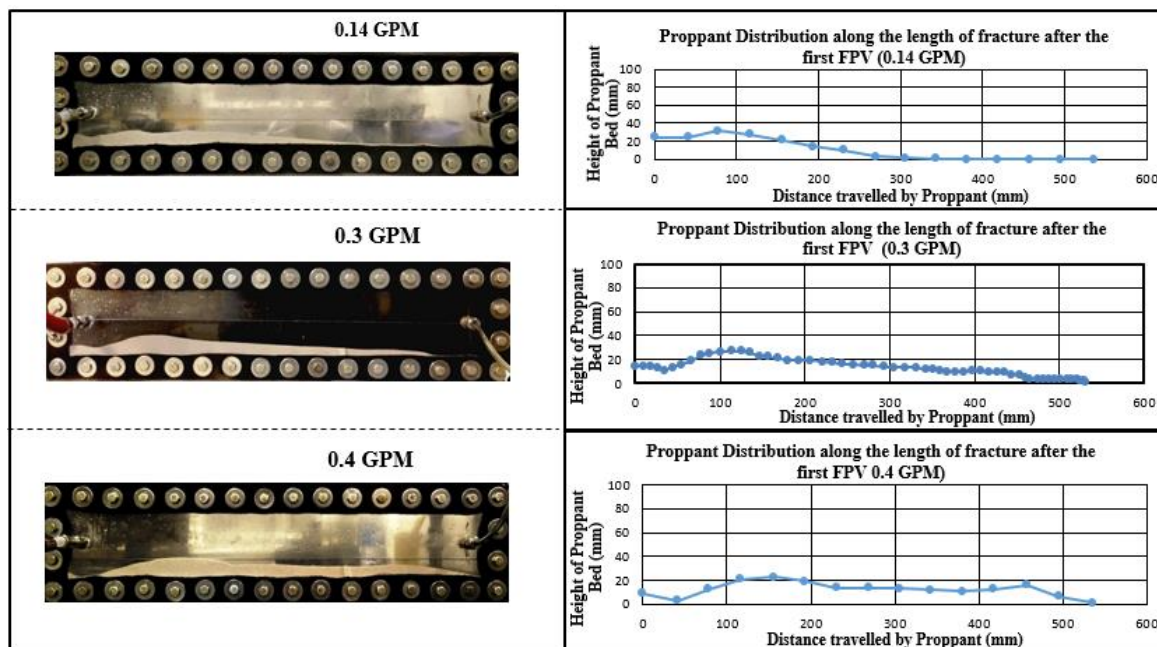


Figure 4.2. Proppant distribution at end of FPV 1 for different flow rates

Figure 4.3. Effect of flow rates on proppant transport in terms of bed height provides a comparison of distribution pattern of proppant at the end of FPV1 for all the three flow rates used in this study.

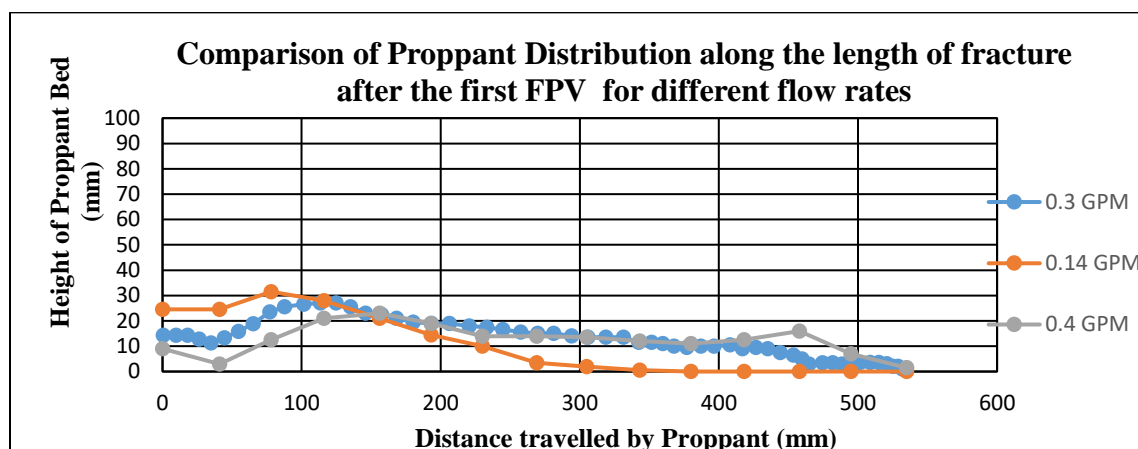


Figure 4.3. Effect of flow rates on proppant transport in terms of bed height

Figure 4.4. Comparison of bed heights for different flow rates at equilibrium shows the comparison bed heights for different flow rates at equilibrium stage. The distance to which the proppant has travelled in plotted along the x-axis and the height of proppant bed is plotted along the y-axis.

It was observed that with an increase in flow rate, the equilibrium bed height decreases. The decrease of bed height is due to increase of flow rates pushing the proppant to exit from the outlet of the parallel plate apparatus. The greater the flow rate, greater is the slurry velocity that was obtained at the top of proppant bed causing a greater decrease in proppant bed height.

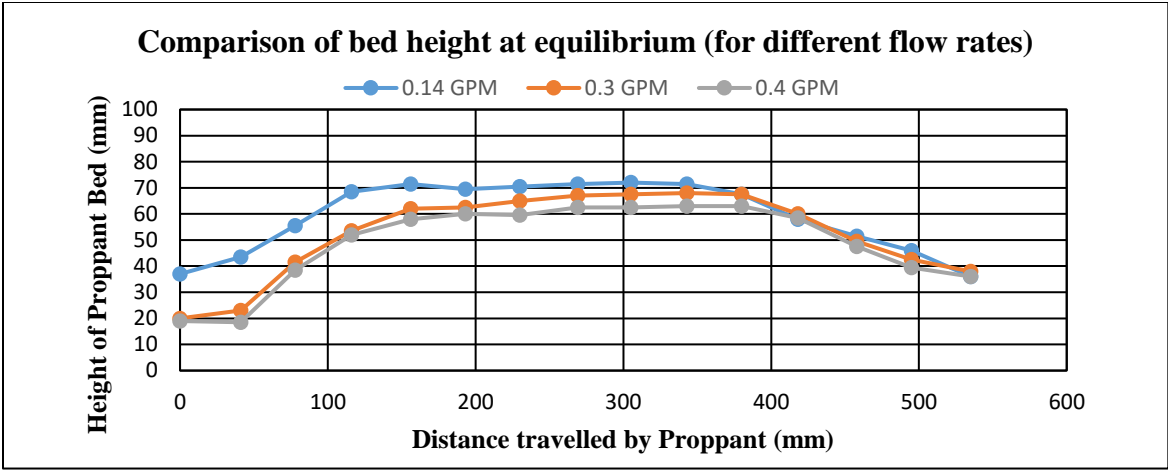


Figure 4.4. Comparison of bed heights for different flow rates at equilibrium

Increase in flow rates from 0.14 GPM to 0.4 GPM has resulted in decrease of equilibrium dune height 86.14% to 75.9%. (See Figure 4.5)

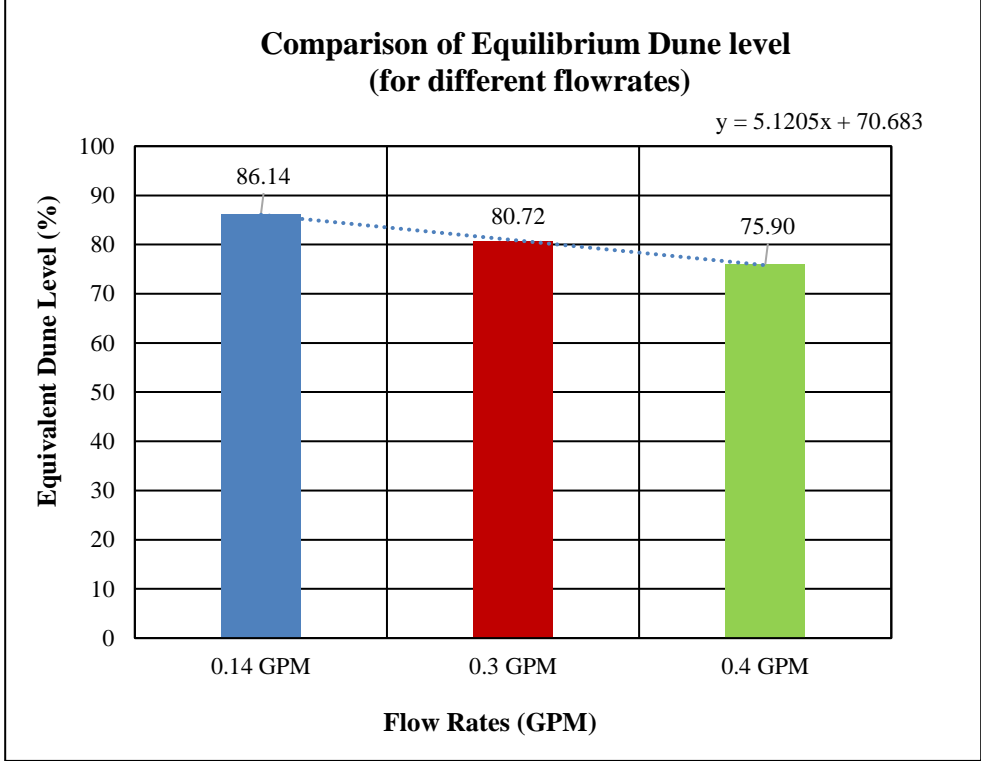


Figure 4.5. Comparison of equilibrium dune level (for different flowrates)

Alataobi et al.2015 observed that for 30/70 brown sand had EDL levels ranging from 90-95% for a concentration of 1 lb/gal. An increase in flow rates/slurry velocities to 80% resulted in a decrease of 5% EDL height. Our experimental observations had a decrease of 4.82% of EDL with an increase of 80% slurry velocities. However, the ranges of EDL's for Ceramic 40/70 Low-density proppant seem to be less that of 30/70 brown sand indicating better transportability of low-density proppant for Slickwater.

Figure 4.6 show the proppant bed heights at equilibrium. The height of proppant bed show that higher the flow rate, greater is erosion leaving more gap above the proppant bed as shown. The setting pattern for all the flowrates had a similar shape as seen.

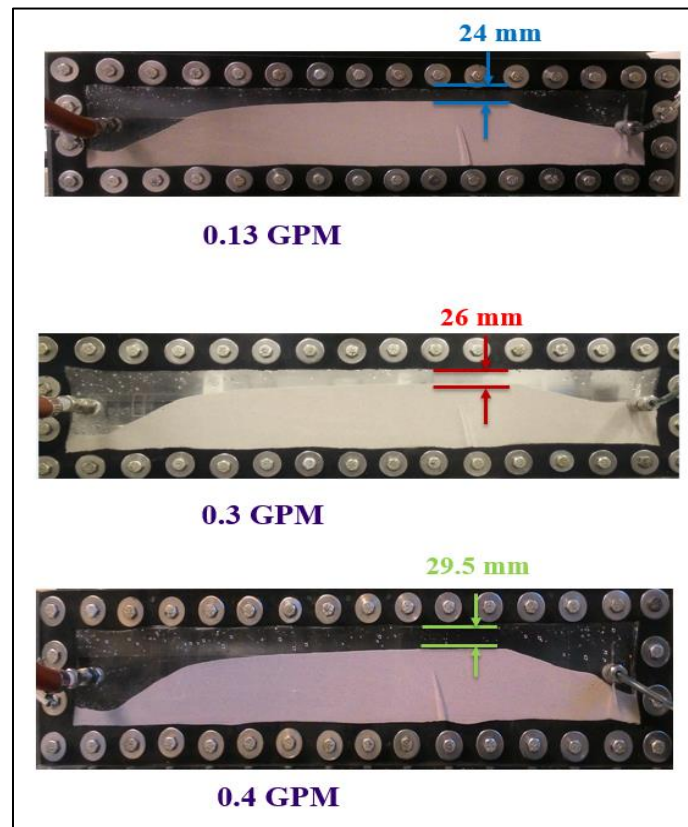


Figure 4.6. Comparison of bed heights at equilibrium

Figure 4.7 shows the surface area fraction of proppant occupied after each run at different flow rates. Higher the flow rate, lesser is the proppant surface area obtained as the greater flow rates cause the proppant to push towards the outlet exiting the plexi glass setup. Higher flow rates tend to cause erosion in the fractures not allowing the proppant to settle down. This results in lower proppant surface area fraction.

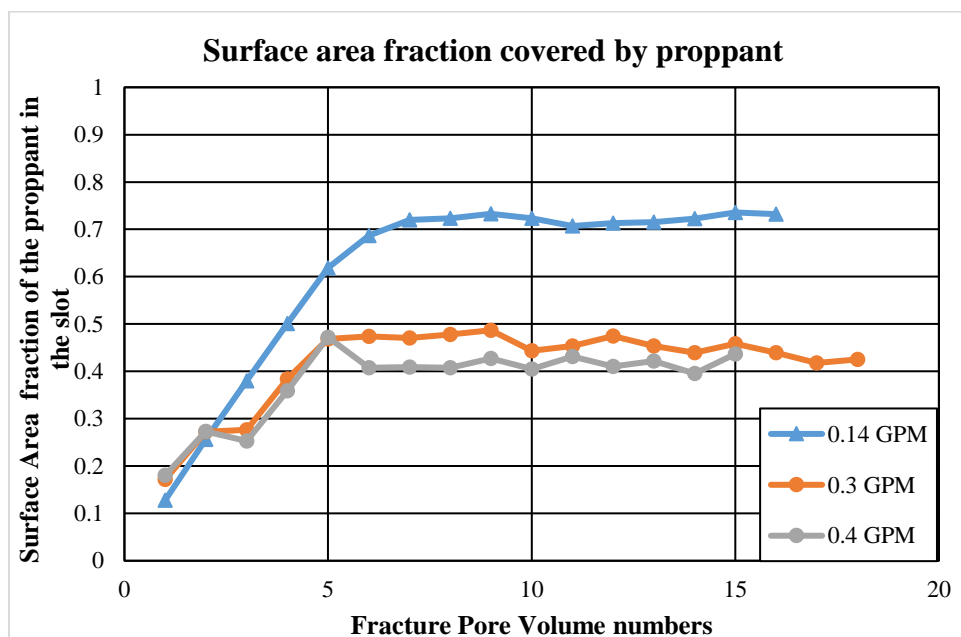


Figure 4.7. Surface area fraction of proppant for different flow rates

Effect of flow rate can be further explained with Figure 4.8. In terms of length, proppant transport can be justified by the numbers of fracture pore volumes required for the proppant to reach the end of fracture and number of runs required to reach the proppant outlet. Figure 4.8 indicates with an increase in flow rate, the number of FPV injections required to reach the proppant outlet reduces. This indicates proppant being transported to greater distances with an increase in flow rates. Also, higher the flow rate,

the lesser was the time taken by the proppant bed to reach equilibrium. This can be illustrated by the number of FPV injections required to reach equilibrium.

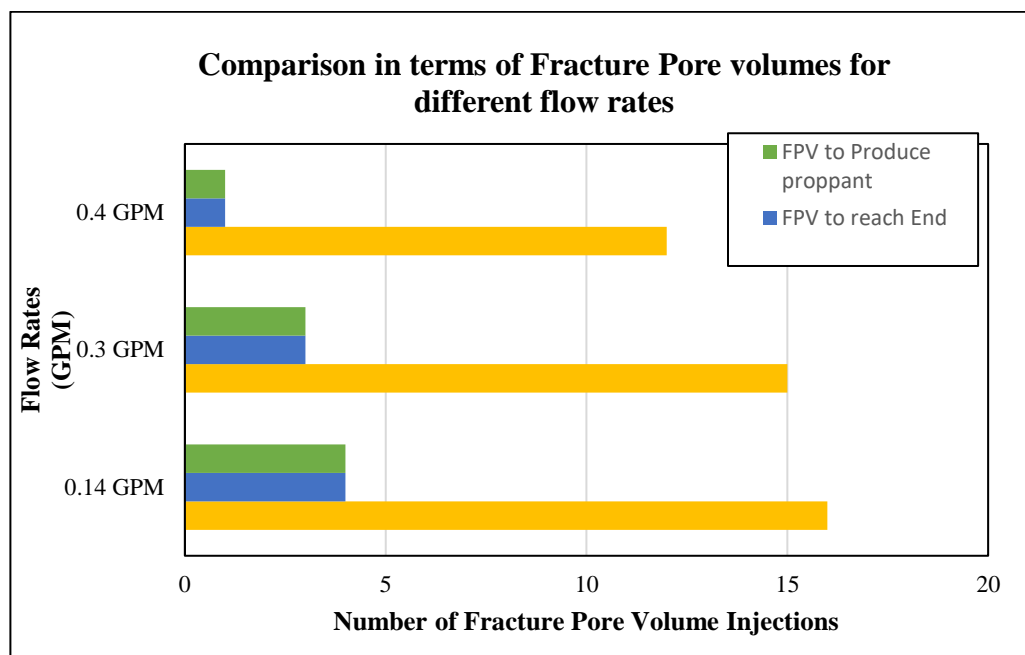


Figure 4.8. Effect of flow rates in terms of number of fracture pore volume injections

4.1.2. Effect of Fracture Width on Proppant Transport. Fracture width is an important factor to address when understanding proppant transport. Experiments included using different fracture width to proppant diameter (W/D) ratios to understand this behavior. We summarize results for different widths at which the experiments were conducted in this study.

Similar to the effect of flow rates on proppant transport, the effect of fracture width can be explained by variables like equilibrium dune length, distance to which proppant has traveled and a number of runs to reach equilibrium. Effect of fracture width

can be explained using Figure 4.9 and Figure 4.10 which represent proppant distribution at end of FPV1 for different widths. We divide these results into two parts based on fracture width to proppant diameter ratio Figure 4.9 is for experiments conducted for W/D ratio around 3 followed by Figure 4.10 which depicts the proppant bed height after injection of FPV1 for a W/D ratio greater than 3. We can see that greater the fracture width, the lesser is proppant bed height as a wider fracture provides more volume for fracture for the proppant to settle.

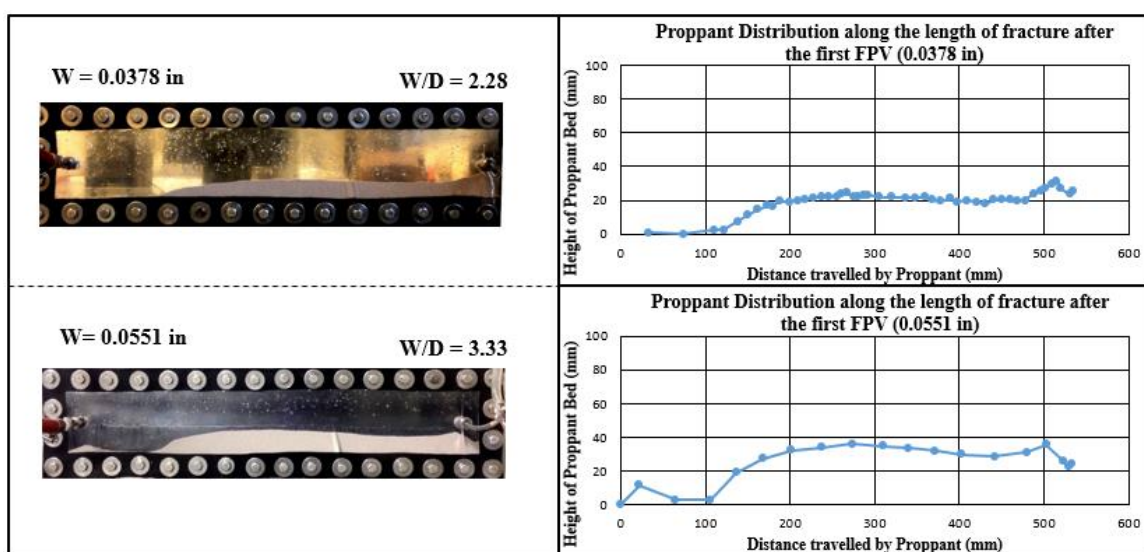


Figure 4.9. Proppant distribution at end of FPV 1 for different widths (W/D ~ 3)

The fracture width of 0.0551 inches has higher proppant bed distributed in the latter end of the fracture slot relative to the proppant bed for 0.0378 inches. In both these cases, due to smaller fracture widths comparable to the diameter of the proppant, no deposition is seen near and around the inlet. This lower width causes greater velocities pushing the proppant deeper into the slot.

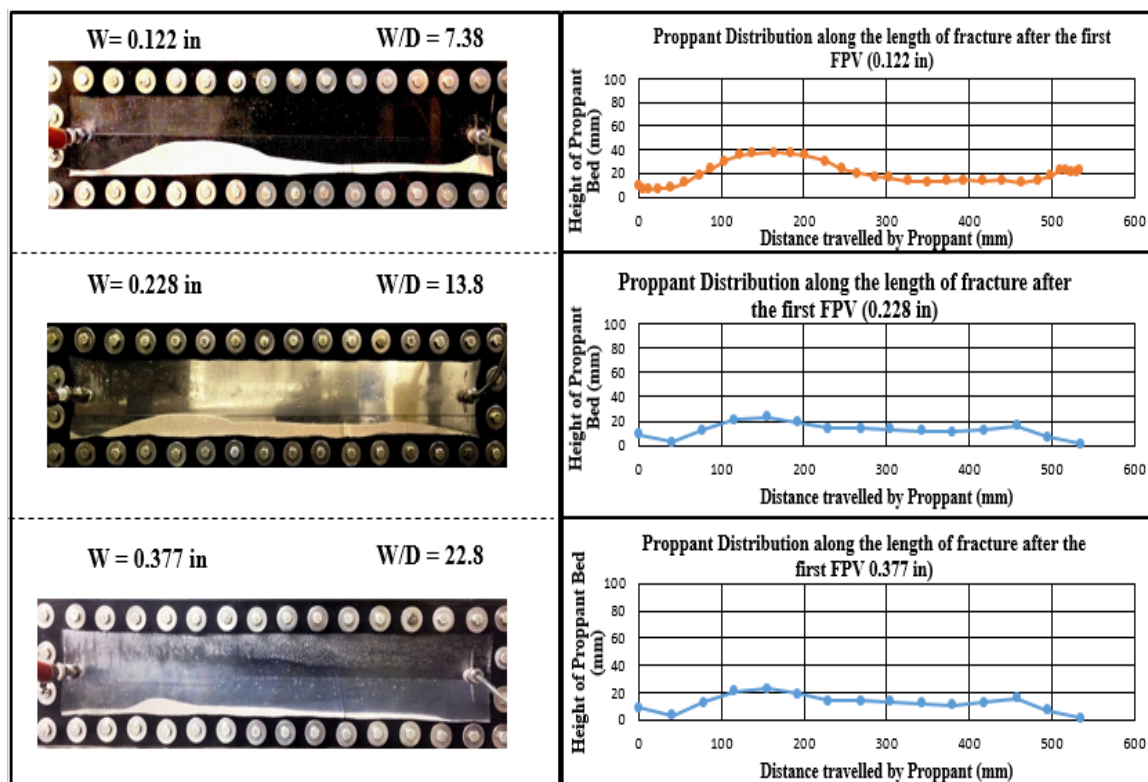


Figure 4.10. Proppant distribution at end of FPV 1 for different widths ($W/D > 3$)

As shown in Figure 4.10, proppant distribution at end of FPV 1 for widths greater than 3, proppant starts settling towards the inlet of fracture slot. After a certain width it was seen that with an increase in width you can see the height of proppant bed decreases. This is due to increase in fracture width the volume of fracture available for proppant to settle is more. As a result, a decrease in proppant bed heights can be seen. In the Figure 4.10, a fracture width of 0.112 inch results in proppant bed height of 39 mm. The highest fracture width of 0.377 inch resulted in a proppant bed height of 22 mm.

Figure 4.11 summarises the height of proppant bed at the end of FPV1 for different fracture widths. Proppant deposition broadly varies based on fracture width.

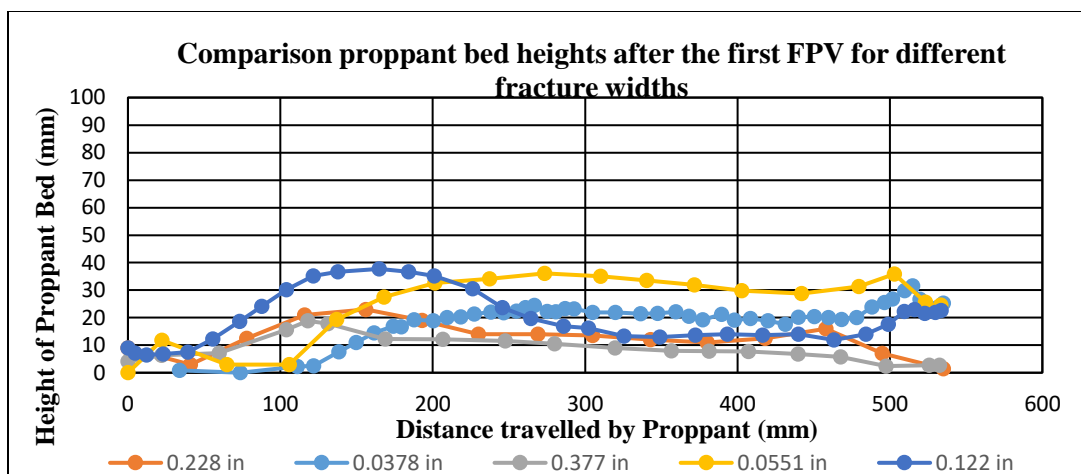


Figure 4.11. Comparison of bed heights at end of FPV 1 for different widths

Figure 4.12. on the other hand indicate that an increase in fracture widths causes an increase in Proppant bed heights at equilibrium. An increase in width between parallel plates increases the area available for the slurry to flow, which in turn decrease the slurry velocities. The decrease in slurry velocities results in proppant being depositing within the fracture slots. This results in higher bed height where there is less erosion of the proppant

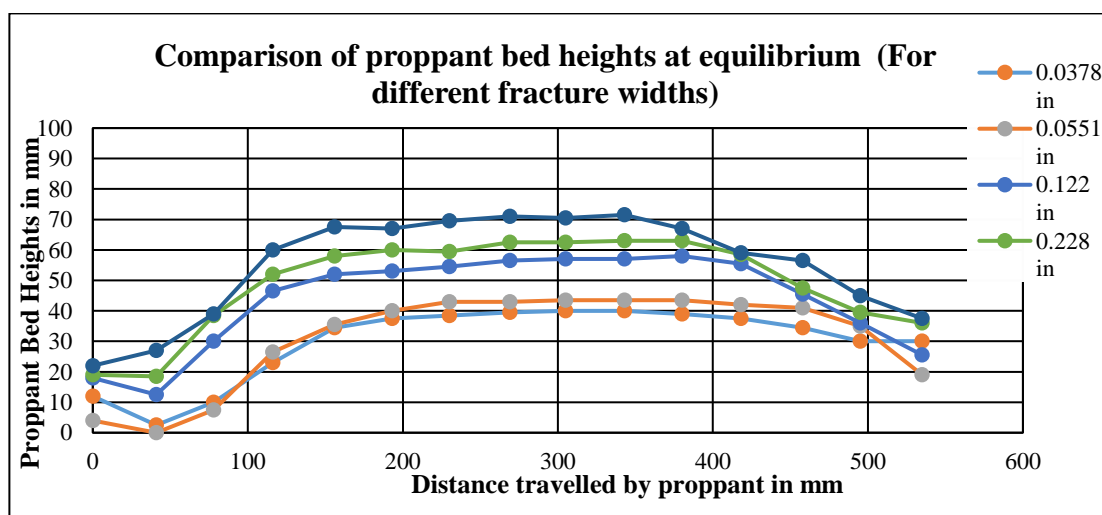


Figure 4.12. Comparison of EDL bed heights for various frac widths

Figure 4.13 indicate with an increase in fracture width bed heights at equilibrium increased significantly. This indicates that most of the proppant transports across the length of fractures and exits the primary slot for lower fracture widths. In addition, the effect of fracture width can be further explained in terms of a number of fracture pore volumes to reach equilibrium. Lower frac widths take lesser time to reach equilibrium and less amount of proppant being settled in the fracture.

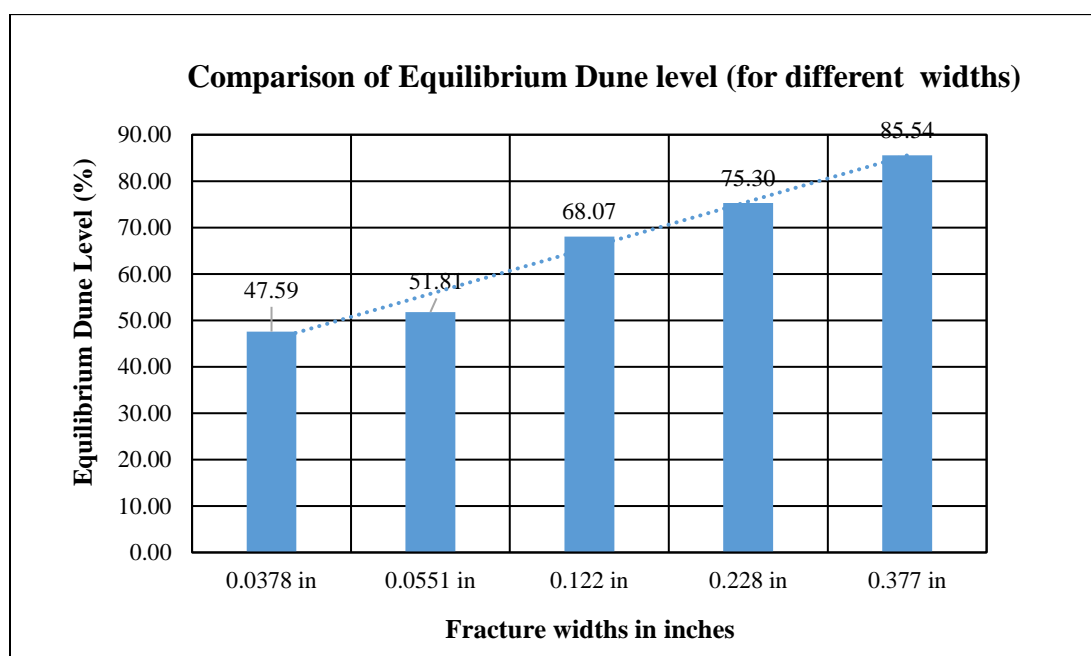


Figure 4.13. Equilibrium dune levels for various W/D ratios

In Figure 4.14, although it is seen that number of FPV injections required to reach the end and that to produce proppant to be same for different fracture widths, the amount of proppant being produced at the outlet at end of 1 FPV injection is different. As the fracture, width decreased the amount of proppant produced at the outlet increased from 1.8 grams to 6 grams. This indicates that more proppant transport along a lower width fracture relative to wider frac width. (For cases where $W/D > 2.5$)

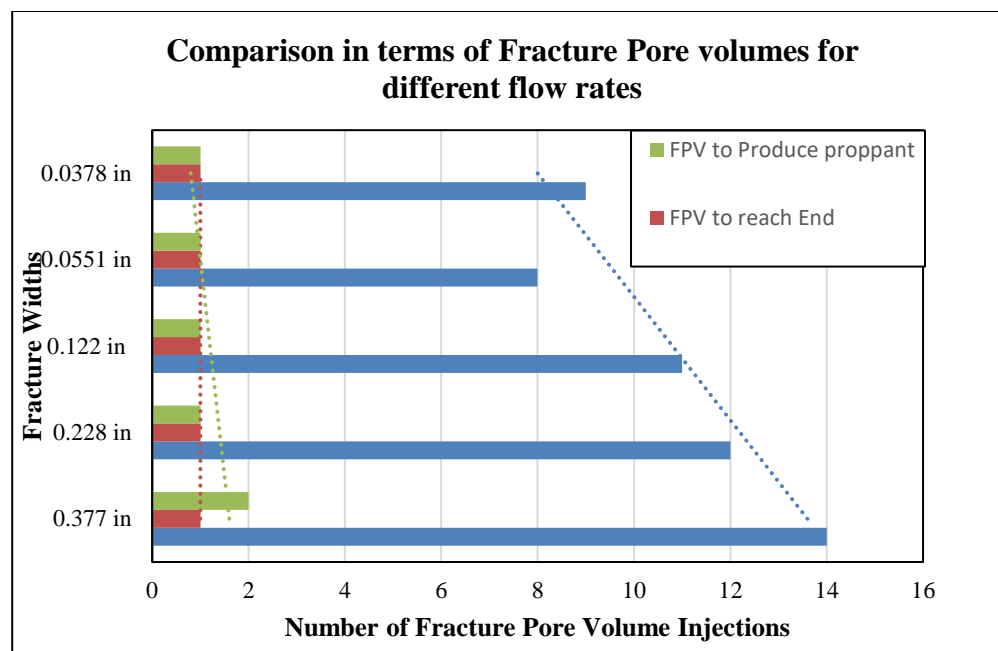


Figure 4.14. Effect of fracture width in terms of number of fracture pore volume injections

4.1.3. Understanding Proppant Transport for W/D Ratio Less than 2.5. Two experiments were conducted in order to study the effect of using very low width of fracture to the diameter of proppant ratio (for a value less than 2.5). Experiments were conducted with the following W/D ratio of 1.18 (~1) and 2.28 (~2). For the study conducted for W/D ratio of 1.18, we observed that proppant was not able to enter the primary fracture slot. Below Figure 4.15 illustrates the inability of proppant to pass by the inlet into the fracture slot. On the left side of the Figure 4.15, we can observe that inlet before the proppant is injected. Figure 4.15 on the right side depicts the inlet after proppant was injected through the accumulator. The water travels into the fracture slot leaving the proppant at the inlet (arrows shown in Figure 4.15). This observation strongly implies that injection of proppant into fracture width which results in W/D ratio ~1 will result in proppant not being able to travel through the fractures.

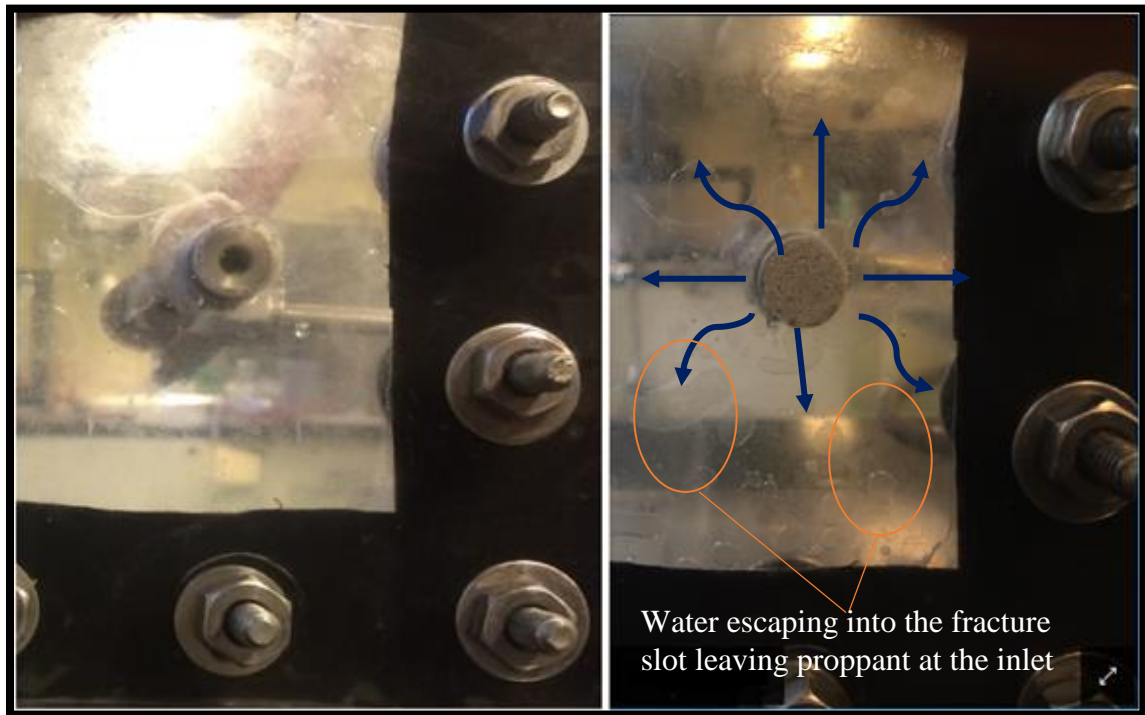


Figure 4.15 Fracture slot showing proppant unable to transport for W/D ratio of 1.18

For the study conducted for W/D ratio of 2.28, we observed that proppant was able to travel through the inlet into the primary fracture slot. Below Figure 4.16 illustrates the dune development pattern for this experiment. We observed proppant showed some resistance to flow in this case due to the low width. The Equilibrium Dune height observed is much lower as this case is the lowest width. This can be explained as low width contributes to lower area fraction for the proppant slurry to flow resulting in greater flow velocities within slots. This results in lesser amount of proppant allowed to settle in the fracture slot and most of it being pushed outwards through the outlet. Also, very less amount of proppant is observed to settle near and around the inlet due to these high velocities observed due to the width change.

This study significantly defies the claims made in previous studies, which state the proppant transport does not occur for a W/D ratio less than 2.5.

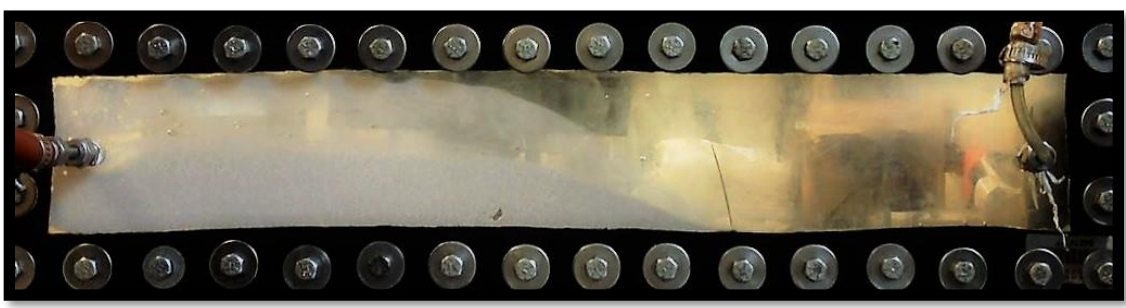


Figure 4.16. Fracture slot showing proppant transport ability for W/D ratio of 2.28

Figure 4.17 shows surface area fraction occupied by proppant within the fracture slot for different widths.

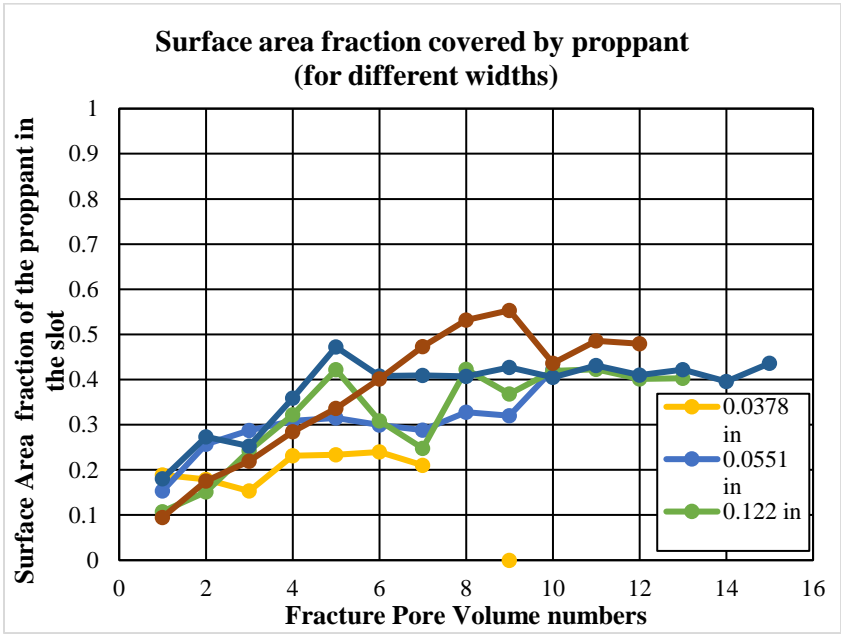


Figure 4.17. Surface area fraction covered by proppant for different fracture widths

An increase in width has resulted in increase in proppant surface area fraction. Highest proppant surface area fraction was seen for fracture with width 0.377 inches and lowest surface area fraction was obtained for 0.0378 inches.

4.1.4. Conclusions for Primary Fractures.

- Effect of flow rates and fracture width on proppant transport has been studied in a unique step-by-step injection process. Each injection of proppant slurry is termed as one 'Fracture Pore Volume'.
- The increase in flow rates decreases in equilibrium dune level. This is due to increased slurry velocities at the top of proppant bed in fracture slots. This increased proppant slurry velocity causes the proppant to move towards the exit of slurry velocity.
- Increased flow rates increase the transport of proppant deeper into the fractures relative to that at lower slurry velocities.
- Proppant slurry at lower flow rates takes greater number of FPV injections to reach equilibrium relative to proppant slurry injected at higher flow rates.
- The increase in fracture width has resulted in an increase in the equilibrium dune levels in fracture slots. The slurry velocities decrease with an increase in cross-sectional area of fracture slot. This results in proppant settling to greater heights and greater proppant surface area fraction.
- The increase in fracture width to diameter of proppant ratio resulted in an increase in the proppant bed heights and an increase in equilibrium dune level.

- It is seen that proppant travel failed to travel into the fracture slot at a W/D ratio of 1.18. However, the proppant was successfully able to travel into the fracture slot for a W/D ratio of 2.28. This study significantly defies the claims made in previous studies which state the proppant transport does not occur for a W/D ratio less than 2.5.

4.2. RESULTS FOR SECONDARY FRACTURES

This Section will discuss the results of experiments conducted using the Secondary fracture apparatus. Understanding the effect of fracture complexity has been an interesting area of research where in multiple studies have been conducted. Previous studies from Sahai et al. 2014, Li et al. 2016, Tong et al. 2016 considered the existence of complexity in fracture networks in their work. These studies covered the effect of parameters like pump rate, proppant loading, proppant size and orientation of secondary fractures. Though these studies were critical in understanding the effect of the above-mentioned parameters, they could not account for step wise distribution of proppant into the secondary fracture. Also, there was very little research done in extending the complexity in terms of the width of fracture. Experiments conducted in this study attempts to provide an insight of proppant transport in complex fracture networks with different primary and secondary fracture widths. This study provides insight to understand the transport of proppant in complex fracture networks characterized of different widths. Results for this studies will be explained in detail in below Section.

4.2.1. Effect of Changing the Width of Primary Fracture. This Section discusses the effect of change in width of primary fracture while keeping the secondary fracture width constant. Figure 4.18 illustrates both the cases used in this study to understand the effect of width of primary fracture on proppant transport. In case 2, primary fracture width is 6.2 mm with secondary fracture width as 5.8 mm. The flow rates in all the above cases are kept constant.

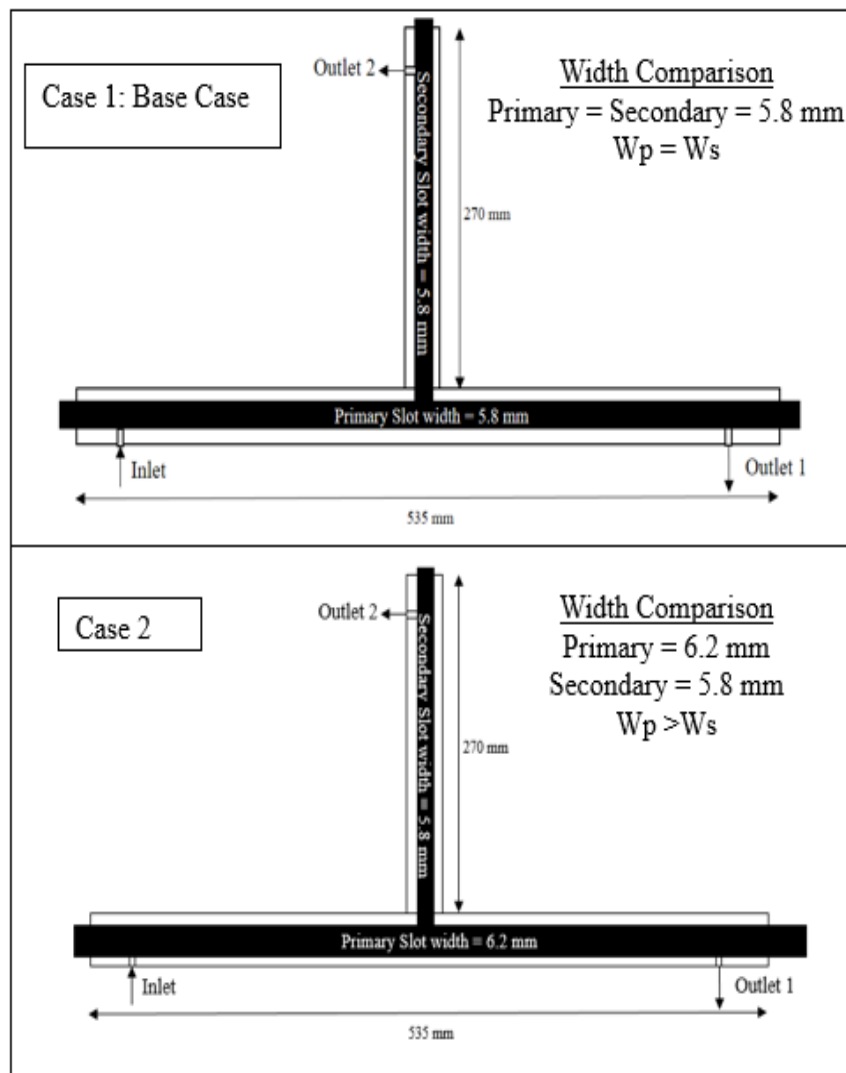


Figure 4.18 Apparatus setup for case 1 and case 2 (top view)

The Figure 4.19 shows the proppant distribution in the primary fracture after injection of FPV 1 for case 1 and case 2. There is no major difference in the distribution for both the cases as seen in tht Figure. A similar observation was seen in the case of proppant distribution in the secondary fractures at the end of FPV1.

The height and distance to which proppant has travelled is identical in both the cases. This observation is illustrated in the Figure 4.20. The proppant bed height in primary slot for both the cases reached to a height of 20 mm where as in the secondary slot proppant bed heights reached to 11 mm. Proppant was seen to reach the end of both primary and secondary slot as illustrated in the Figure 4.19 and Figure 4.20.

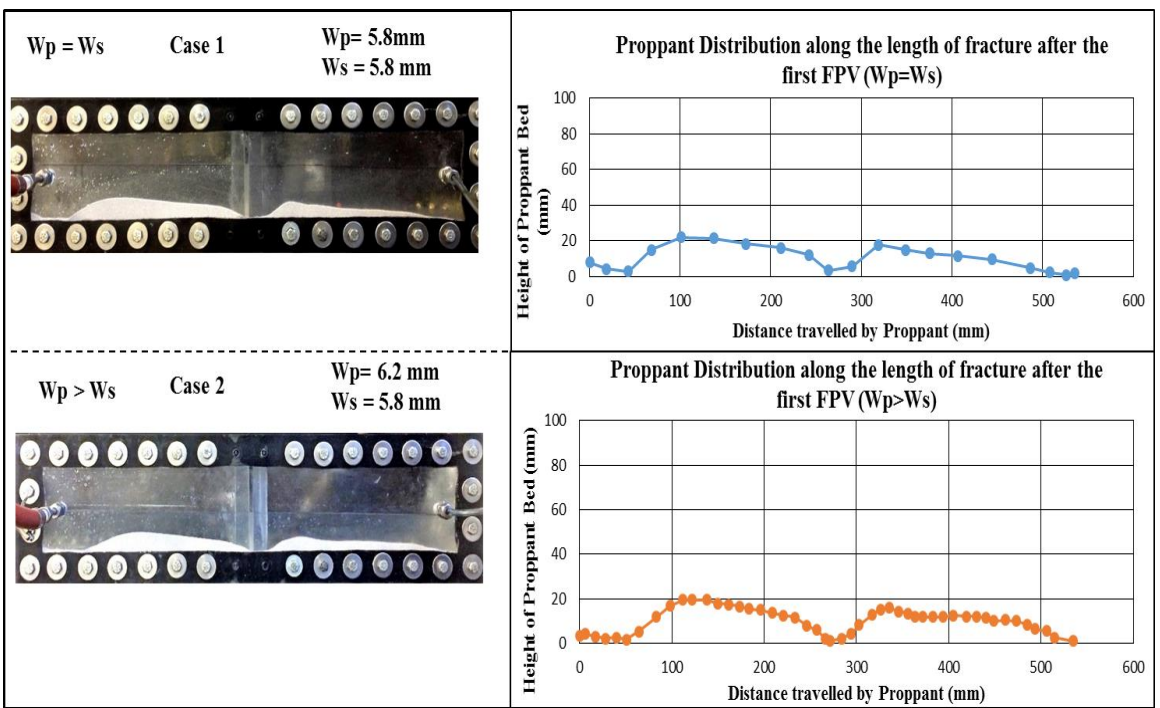


Figure 4.19. Proppant bed at end of FPV 1 (primary slot) case 1 and case 2

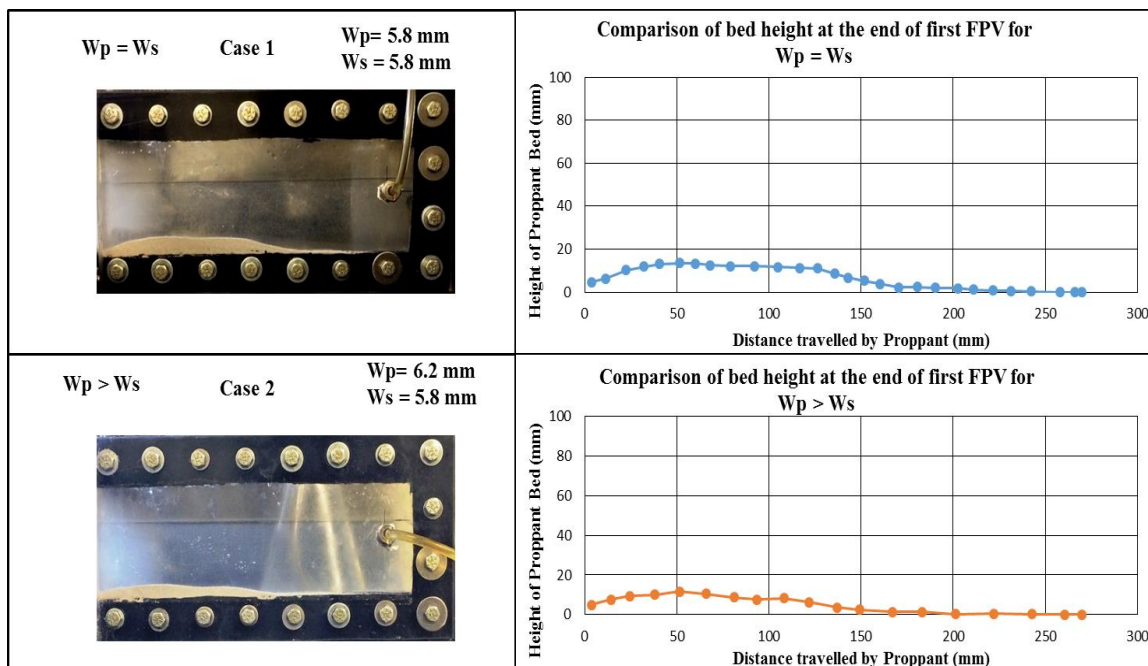


Figure 4.20. Proppant bed at end of FPV 1 (secondary slot) case 1 and Case 2

At equilibrium proppant distribution has shown a significant change unlike the distribution seen at the end of FPV 1. Proppant bed heights has seen an increase in both, primary and secondary fractures. This difference in distribution of proppant in primary and secondary fractures for case 1 and case 2 are evident in Figure 4.21 and Figure 4.22. Major change in the heights of proppant bed was observed in second half of primary fracture as the proppant travelled across the secondary fracture entrance Figure 4.21

An increase in proppant bed height for secondary fracture was seen. This can be attributed to a significant decrease in slurry velocities as the fluid flows from wider primary slots and turn into secondary fracture.

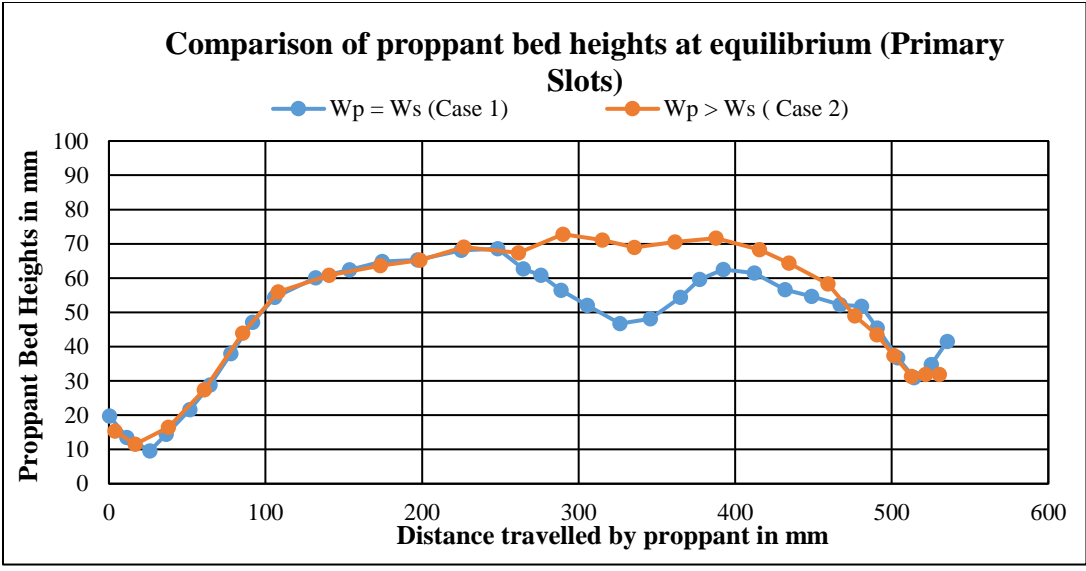


Figure 4.21. Proppant bed heights at equilibrium in primary slot (case1 Vs case2)

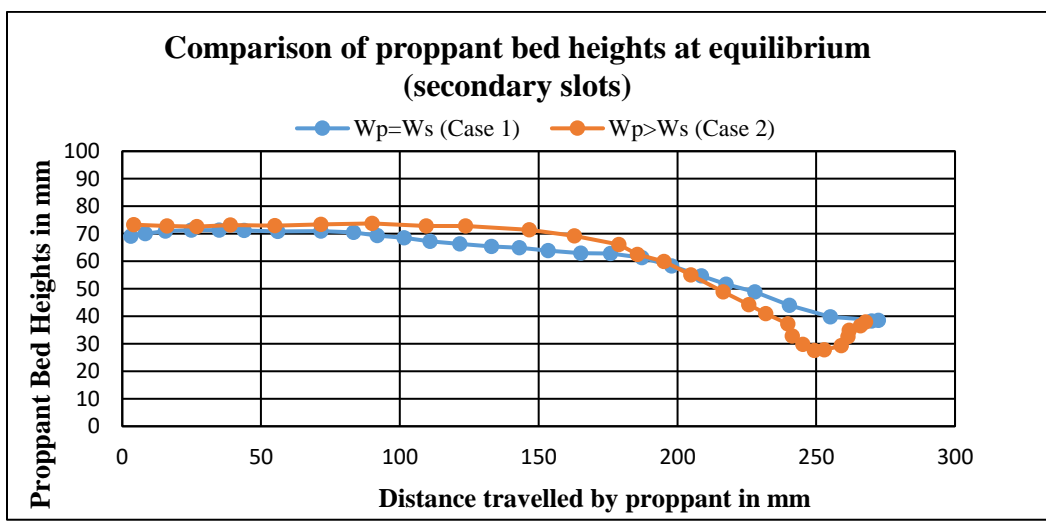


Figure 4.22. Proppant bed heights at equilibrium in primary slot (case 1 vs case 2)

As mentioned in the earlier Section, a consequence of difference in bed heights observed at equilibrium for case 1 and case 2 is the difference in equilibrium dune level. The equilibrium dune level for primary and secondary fractures in both the cases are presented in the Figure 4.23. It can be seen that the equilibrium dune levels increase in both primary and secondary fractures in case 2 relative to that of case 1. This implies

increase in primary fracture width has resulted in increase in equilibrium dune levels in primary and secondary fractures. Equilibrium dune level increased by 4.7% in primary fracture and by 5.4% in secondary fracture.

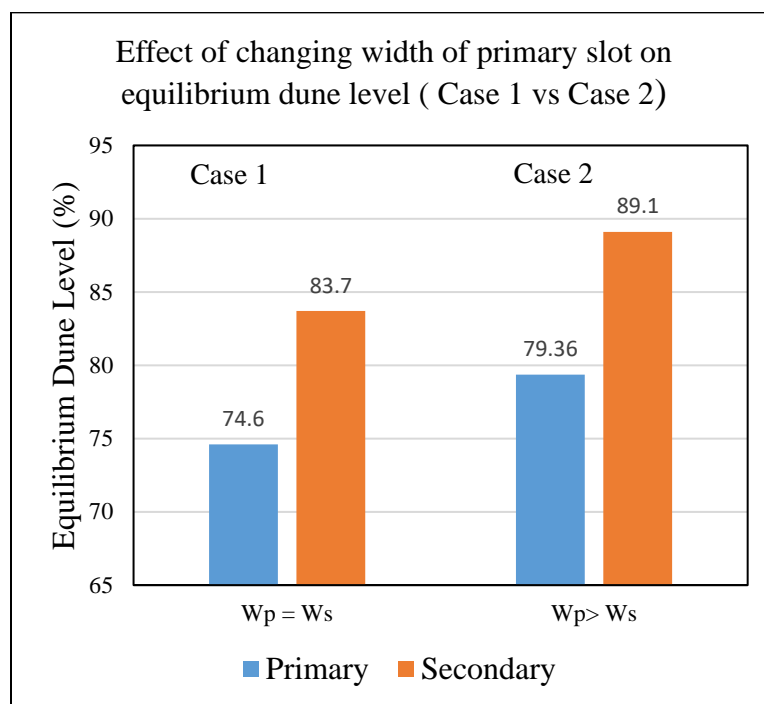


Figure 4.23. Comparison of equilibrium dune levels in primary and secondary slots

4.2.2. Effect of Primary Fracture Width Heterogeneity. This Section discusses the results obtained for the study of effect of primary fracture width heterogeneity on proppant transport. As mentioned above, proppant transport in complex fracture networks with heterogeneous fracture width has been studied limited previously. Dhurgham et al. 2017 have studied the effect of heterogeneity of fracture width on proppant transport in single primary slots. This study need to be extended to complex fracture networks. The design of the parallel plate apparatus was modified to accommodate the heterogeneity of fracture width in the secondary configuration. Figure

4.24 illustrates the schematic top view of apparatus for the base case/case1 and the case 3 with width heterogeneity. Case 3 in the Figure 4.24 shows a change in the width of primary slot occurs at half the length of the primary slot. The width heterogeneity ratio i.e. ratio of width at the inlet to the width at the outlet of primary slot is 2. The primary slot width at the inlet in 6.2 mm and at the outlet it is 3.1 mm. The secondary slot width was 5.8 mm similar to that of case 1. Please note that the flow rates and concentrations used in both the cases are constant.

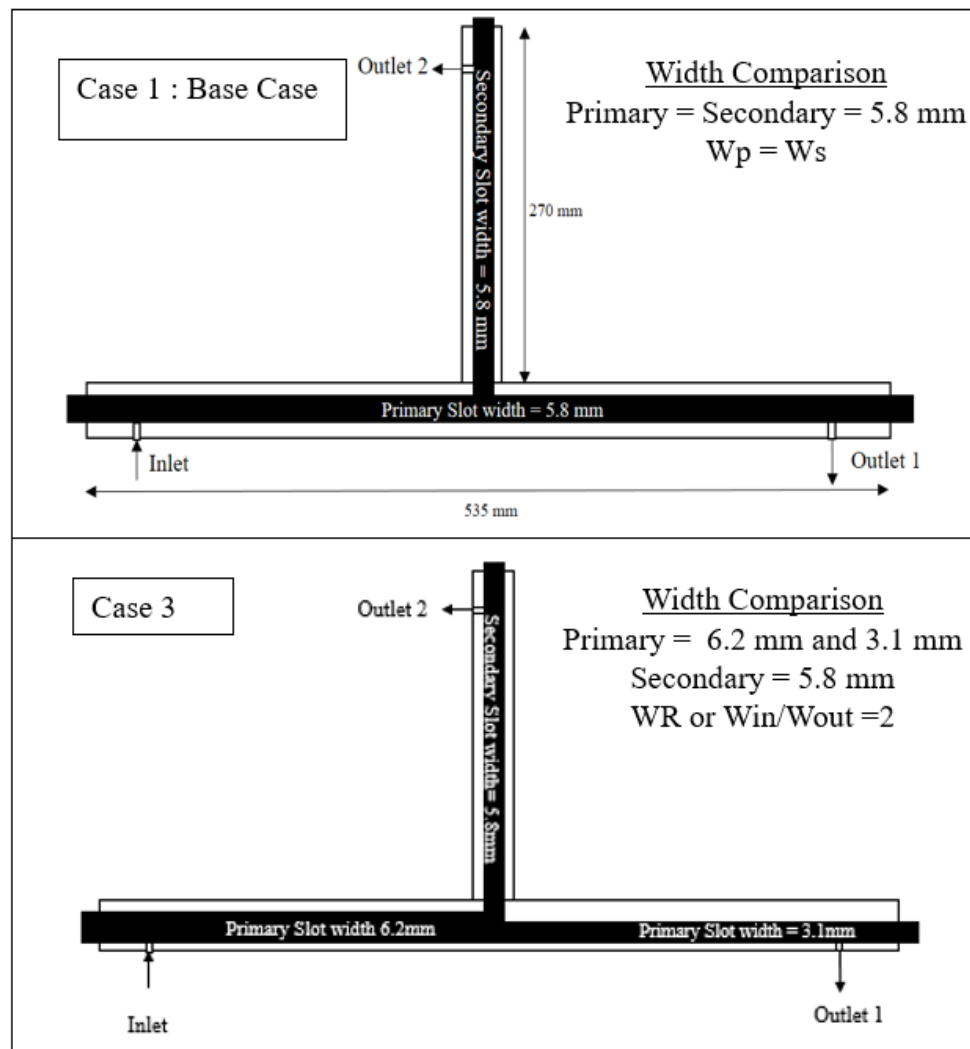


Figure 4.24. Apparatus setup for case 1 and case 3 (top view)

Figure 4.25. Proppant bed at end of FPV 2 (primary slot) for case 1 and case 3 show the distribution of proppant along the primary fracture at end of injection of FPV 2 for both the cases. It was seen that the proppant distribution in both of the cases was similar. There was no major difference observed in the proppant distribution for the case 3 relative to the base case. A Similar observation was seen in the proppant bed heights in secondary slots. This can be seen in Figure 4.26.

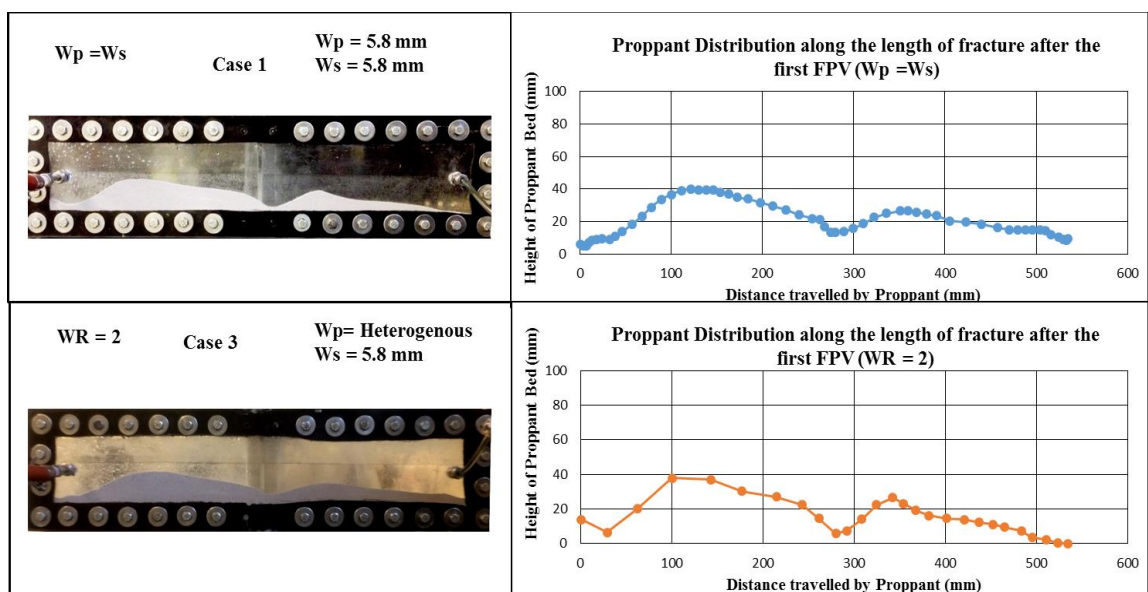


Figure 4.25. Proppant bed at end of FPV 2 (primary slot) for case 1 and case 3

Comparison of proppant bed heights at equilibrium in primary slots from case 1 and case 3. Proppant distribution was different for case 3 relative to the case 1. Proppant bed height slightly higher for case 3 relative to that of case 1. This is evident in Figure 4.27. A comparison of bed heights in the secondary fracture at equilibrium is shown in the Figure 4.28. A very slight increase in bed height was noted in case 3 when compared to case 1 in the secondary fracture.

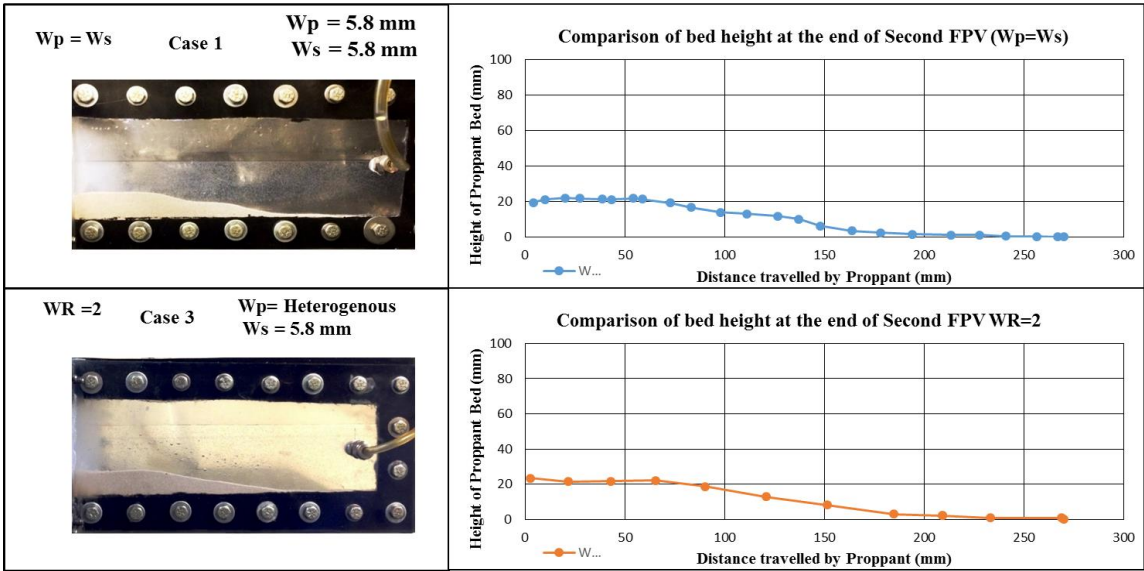


Figure 4.26. Proppant bed at end of FPV 2 (secondary slot) for case 1 and case 3

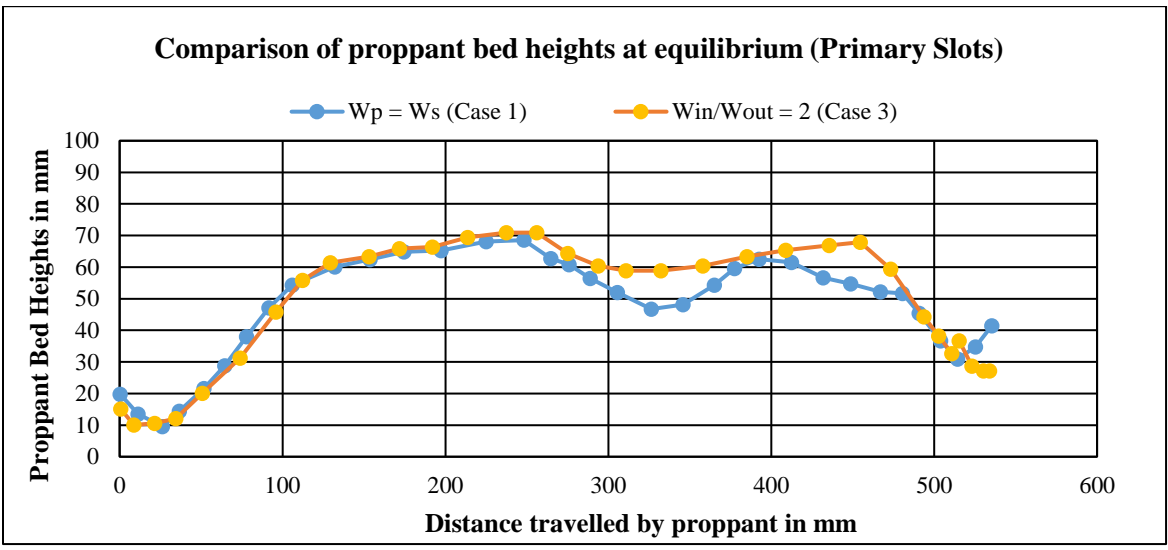


Figure 4.27. Comparison of proppant bed heights in primary slot (case 1 vs case 3)

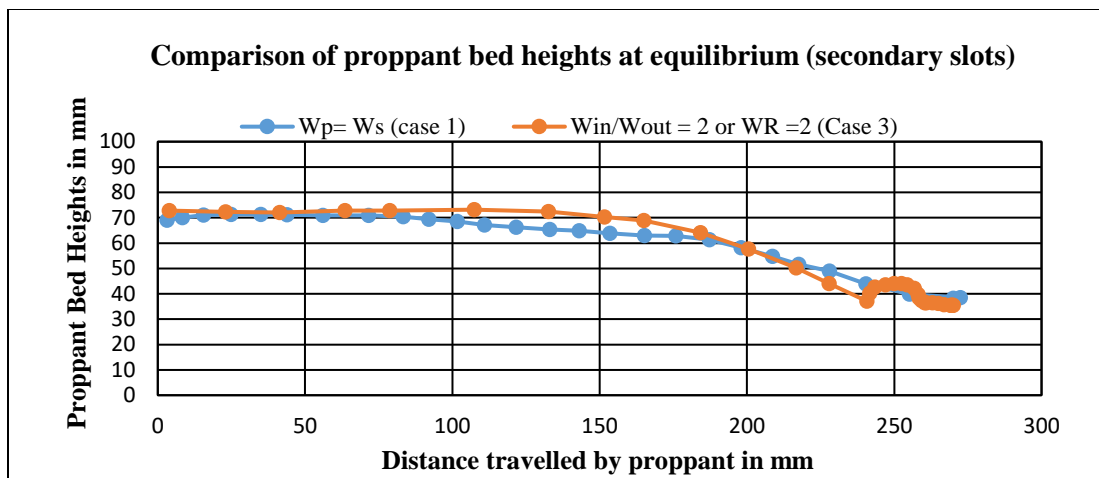


Figure 4.28. Comparison of proppant bed heights in secondary slot (case 1 vs case 3)

A comparison of equilibrium dune levels in primary and secondary fractures for case 1 and case 3 are presented in Figure 4.29. It was seen that equilibrium dune levels were higher in both primary and secondary fractures in case 3 when compared to that of case 1. Equilibrium dune level increased by 8.7% in primary fracture and by 5.5% in secondary fracture.

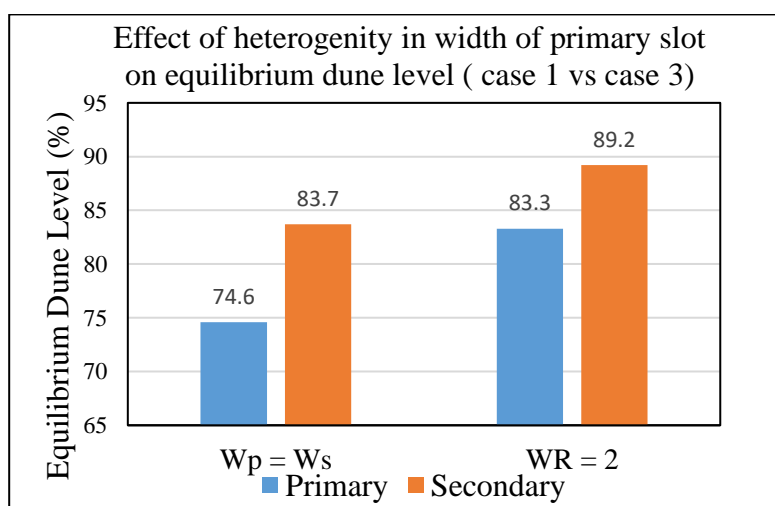


Figure 4.29. EDL bed heights in primary and secondary slot (case 1 Vs case 3)

Results from Figure 4.30 and Figure 4.31 indicated the surface area fraction occupied by proppant in primary and secondary slots respectively for case 1, 2 and case 3. Discussing the proppant deposition in primary slots, in Figure 4.30 it was seen that heterogeneity results in greater proppant being deposited within the primary fracture slot, hence greater surface fraction of proppant was seen for this case. The grey line in the Figure 4.30 represent the proppant area fraction the case with heterogeneity. Higher followed by the case with a wider primary fracture (orange line in the plot). Base case has the least proppant surface area fraction.

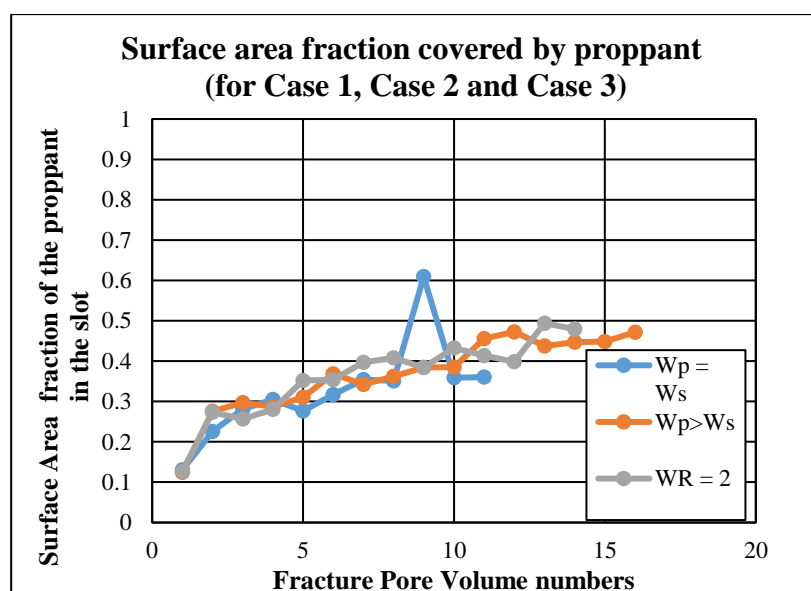


Figure 4.30. Surface area fraction for primary slot (case 1, case 2 and case 3)

Surface area fraction for secondary slots remain same in all three cases indicating no major affect of changing primary fracture width and heterogeneity.

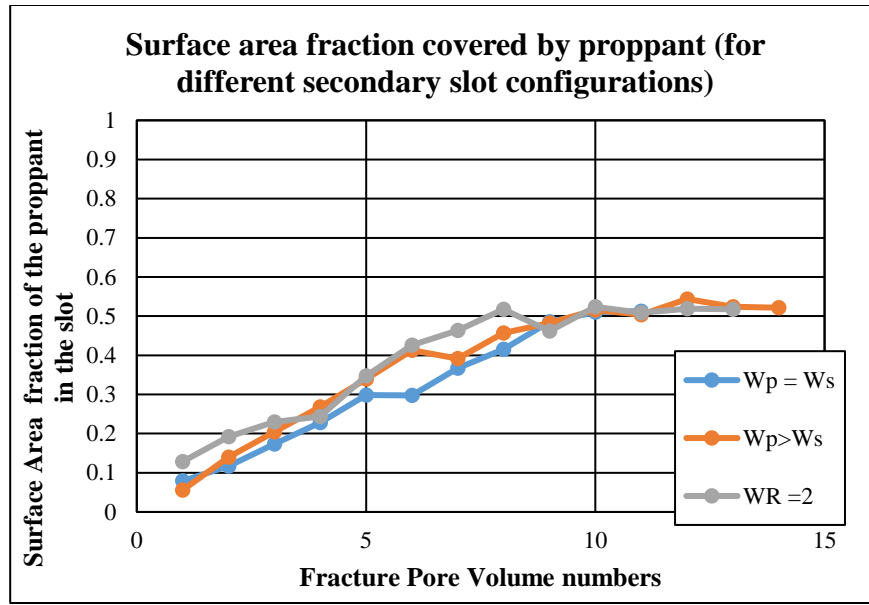


Figure 4.31. Surface area fraction for secondary slot (case 1, case 2 and case 3)

4.2.3. Conclusions for Secondary Fracture Apparatus.

- In complex fracture networks, The width of the primary slot and secondary slot have a significant effect on equilibrium dune level
- With an increase in primary slot width, there is an increase in the equilibrium dune levels of both primary and secondary fractures. This can be due to increase in width causing a greater flow area and lesser slurry velocities within the fractures.
- In the case of an increase in primary slot width, the proppant distribution was affected majorly in the secondary fractures. The change in distribution in the case of primary fracture was seen only after the proppant has passed past the secondary slot.
- Heterogeneity in fracture width of primary slot also had a notable effect on the distribution of proppant in complex fracture networks.

- Heterogeneity in primary slot fracture width has resulted in an increase in the equilibrium dune levels and an increase in proppant surface area fraction for primary fractures. There was no change seen in case of secondary fractures

4.3. PARTICLE SIZE DISTRIBUTION ANALYSIS

This Section will discuss the particle size distribution of proppant within primary and secondary fractures. These analysis were performed in order to understand how proppant particles of different sizes travel across fracture networks. Microtrac S3500 particle size analyser was used to study the particle size distribution in fracture networks. The experimental apparatus was divided into three parts for better understanding of proppant particle distribution as shown in the Figure 4.32.

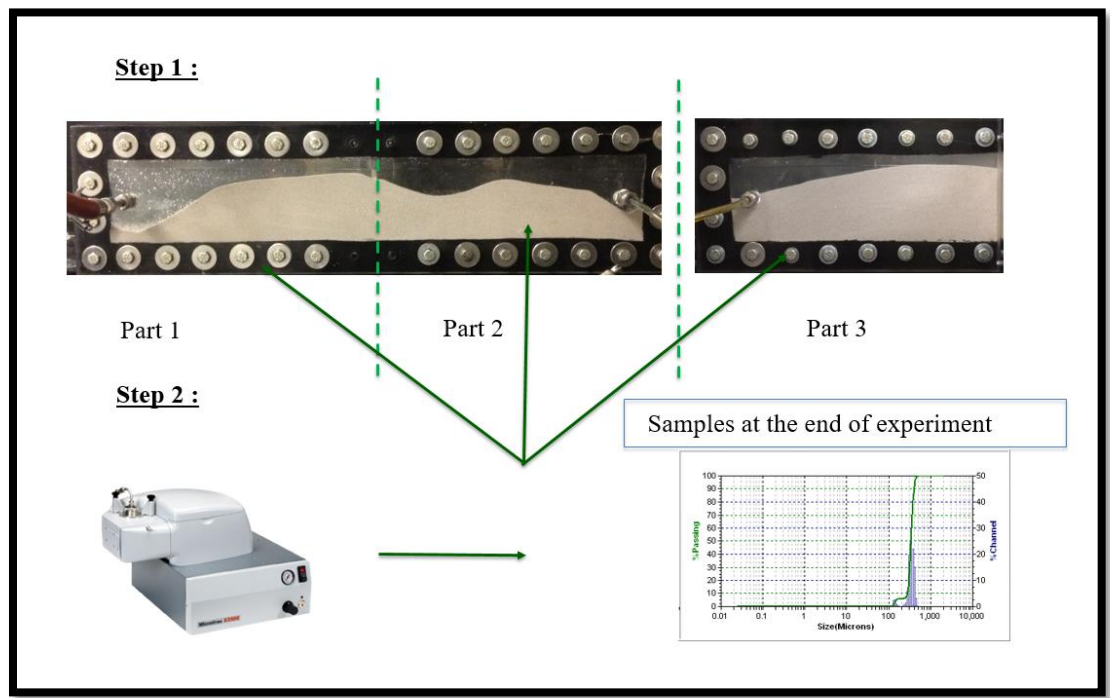


Figure 4.32. Particle size distribution analysis

Steps to perform particle size dimension analysis involve collection of two to three samples of proppant from each of the three parts of the apparatus. These samples are collected in vacuum-sealed containers to avoid any contamination. Later these samples were introduced in particle size analyser with distilled water.

The particles were subjected to ultrasonic vibrations to make sure no particles are stuck with each other during analysis. This provides more precision and accuracy in the results. The particle size analyser performs the analysis measuring the range of particles present within the current sample. The output is provided in the form of graph plotted with size on x-axis and sample volume percentage passing on the Y-axis.

To understand the results obtained from a particle analyser, an example is shown in Figure 4.33. The three orange lines represent the diameter at which given volume percentage of particles can pass through and is usually used to represent the size distribution of particles.

The D50 is the diameter at which 50% of the sample's mass is comprised of particles with a diameter less than this value. Similarly, D90 is the diameter at which 90% of the sample's mass is comprised of particles with a diameter less than this value. D50 is also called the median diameter of given sample. Particle size analyser also presents results for diameter with peak volume % and mean diameter.

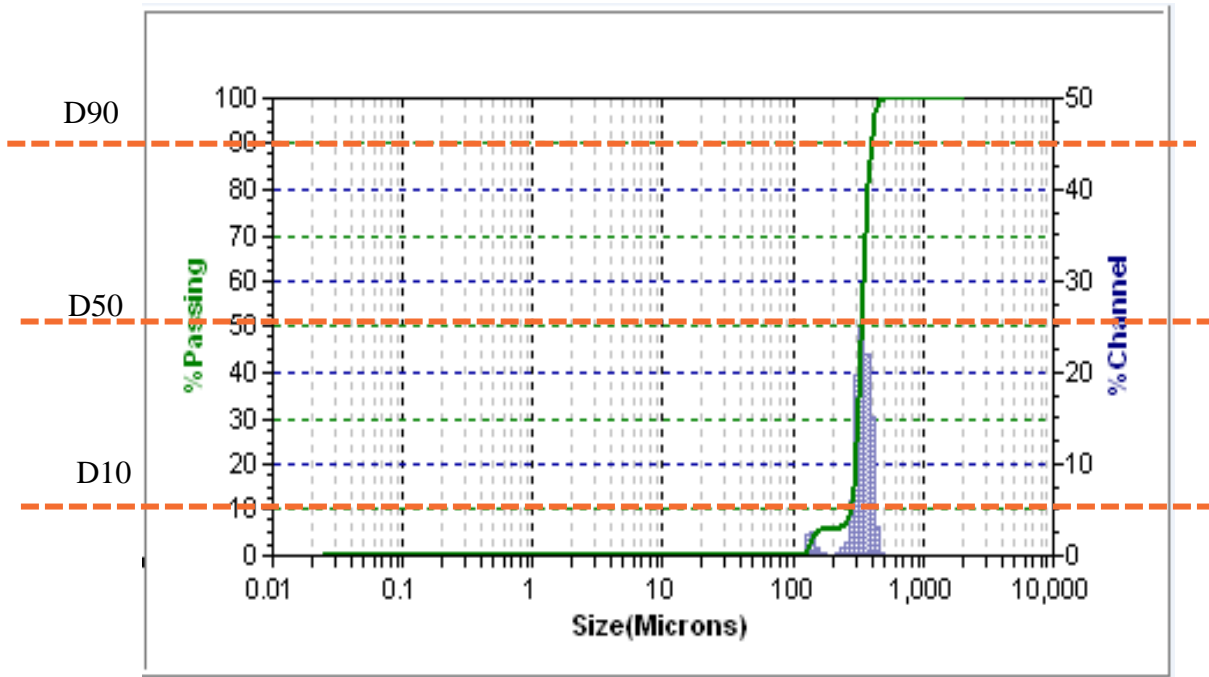


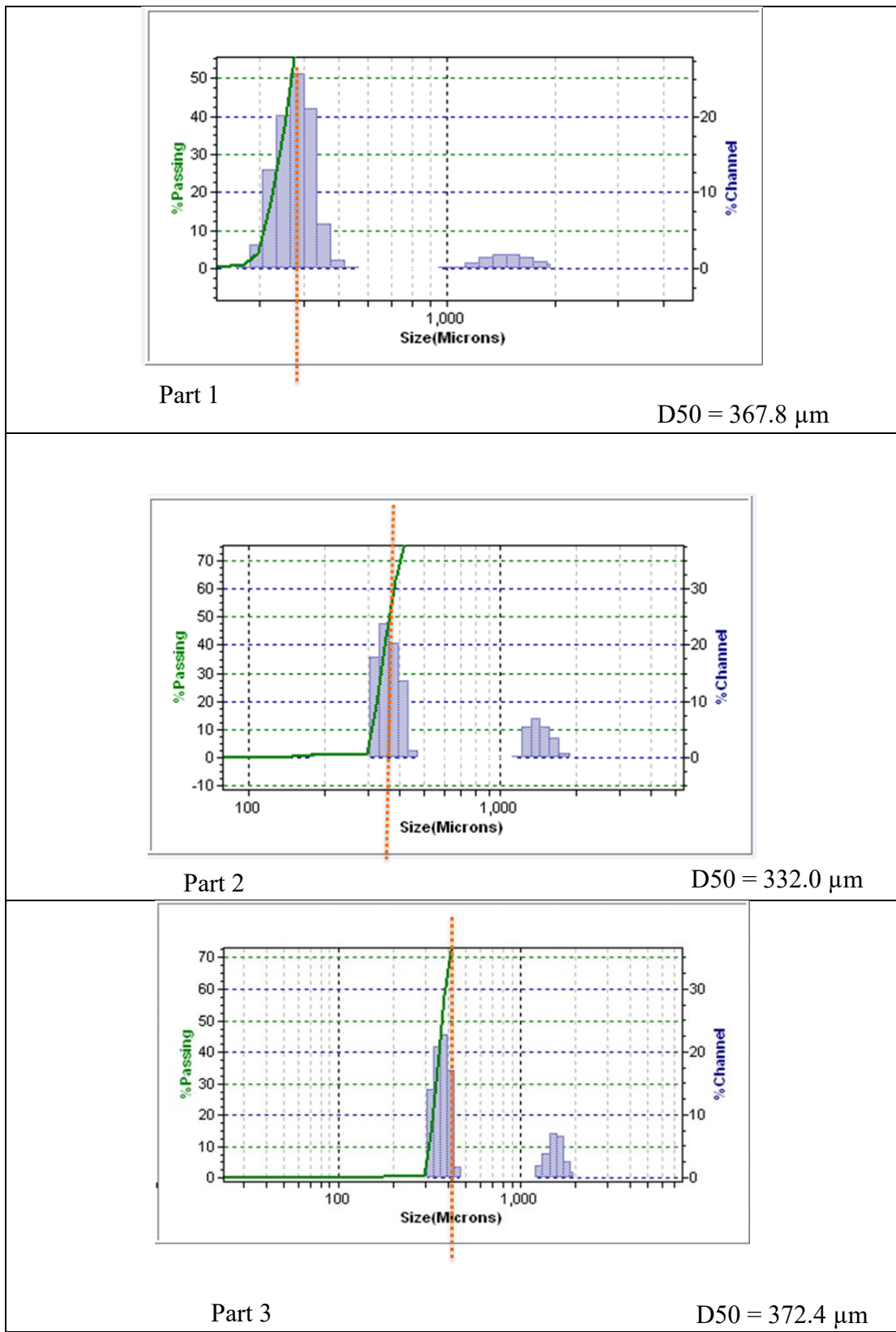
Figure 4.33. Example of results obtained from particle size analyser

We performed the particle size dimension analysis for case 1 of our experiments where the primary and secondary fracture were of same width. The results are summarised below in Table 4.1 and Table 4.2.

Table 4.1 shows the particle size distribution curve for the samples collected for three parts as mentioned above for case 1. As mentioned above, the x-axis has the particle mesh sizes measured in microns and y-axis shows the percentage of particles passing for a given mesh size.

It was seen that part1 of the primary fracture had a D50 of 367.8 μm , the part 2 had a D50 of 332 μm and the secondary fracture (part 3) had a D50 of 372.4. The outliers can be observed beyond 1000 μm .

Table 4.1. Results for particle size distribution analysis (D50) for Case 1



In addition, the diameter of particle with its peak volume % are shown in Table 4.2. Summary of results for particle size analysis. The diameter with peak volume percentage indicate that part 1 has maximum volume of large particles (90.90% of the diameter 362.2 μm). The secondary fracture peak volume percentage 76.6 % with a particle diameter of 356.6 μm and smallest particles were found in part 2 of primary fracture with a diameter of 337.6 μm and volume percentage 87%.

Table 4.2. Summary of results for particle size analysis

Fracture Part	Primary Part(1)	Primary Part (2)	Secondary
Particle Distrubution (SD) %	0.49	0.367	>5
Diameter (Peak Volume %)	362.2 (90.90 %)	337.6 (87%)	356.6 (76.6%)
D 50 Diameter	367.8	332	372.4
Mean Diameter (μm)	381.3	412	428.1

Particle distribution reference chart is presented in Table 4.3. Ceramic proppant used in this study having high sphericity and roundness fall under the category of well sorted. However, the results could not be verified due to the limitations of apparatus availability. Verifying these results will make the results more reliable and can be helpful in determining the size distribution of particles within a fracture. This work can be extended to future laboratory scale studies and is greatly recommended.

Table 4.3. Reference terminology for particle distribution

SD_g Value	Terminology
0.35	Very well sorted (Very narrow)
0.35 - 0.5	Well sorted
0.50 – 0.710	Moderately well sorted
0.71 – 1.0	Moderately sorted
1.0 – 2.0	Poorly sorted
2.0 – 4.0	Poorly sorted
> 4.0	Extremely poorly sorted (very broad)

5. CONCLUSIONS

- Effect of flow rates, slurry velocity, fracture width has a significant influence on proppant transport.
- Injection flow rates were found to be significantly affecting the proppant transport within the slots. As the flow rate increases, there is a decrease in the bed heights.
- Studies for W/D ratios more than 3 indicate that with an increase in fracture width, the settling of proppant increases creating higher bed heights.
- There has been a decrease in equilibrium dune level obtained with a decrease in width.
- Proppant transport can be further quantified and described using the distance to which the proppant has traveled across the fracture and number of fracture pore volumes that have been injected to reach the equilibrium stage.
- In case of complex fracture networks, changing fracture width and heterogeneity in primary fracture width has a significant effect on proppant transport
- The increase in fracture width of primary fracture slot or heterogeneity in fracture slot has caused a significant increase in bed heights and equilibrium dune levels.
- Particle size distribution analysis can be helpful in determining how the proppant distributes into the complex fracture networks

6. FUTURE WORK

6.1. EFFECT OF PROPPANT SPHERICITY/SHAPE

There has been a noticeable difference in the equilibrium dune level is obtained from the previous study by Alotaibi et.al, using 30/70 brown sand and present studies using 40/70 ceramic proppant. The difference in EDL may be accounted using multiple reasons such as angular shape and low sphericity of proppant. Figure 6.1 gives an idea of the difference in the settling pattern of proppant relative to that of sand. Understanding the effect of proppant sphericity should be considered an important to predict the transport of proppant. However further experiments should be conducted to confirm if the difference in results occurs due to sphericity.

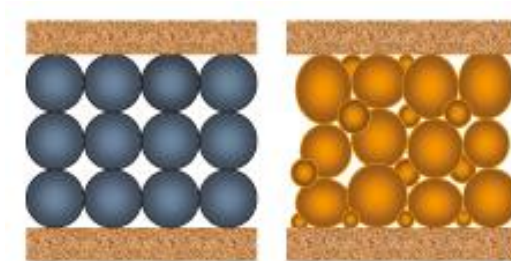


Figure 6.1 Proppant settling with high and low sphericity

6.2. EFFECT OF FRACTURE WIDTH HETEROGENEITY

This study has made an attempt to understand the effect of having fracture heterogeneity in width of the primary slot along with a secondary slot oriented at 90° . Further studies have to be conducted at different widths and different orientation angles of secondary slot to understand the behaviour of proppant transport Figure 6.2 explains the scope of study where the fracture width of primary slots is varied.

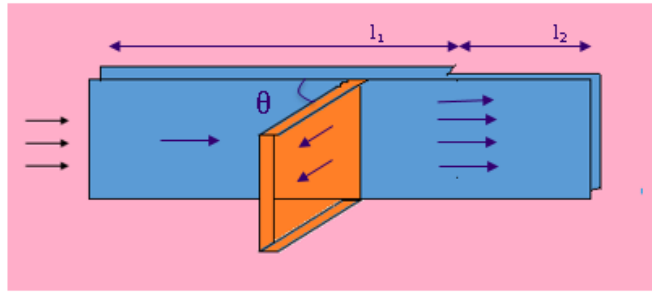


Figure 6.2. Study of heterogeneity in fracture width for complex fracture networks

6.3. PARTICLE SIZE DISTRIBUTION

Particle size distribution analysis of proppant is a novel concept in understanding how proppant particles move into the fracture networks. Its application to laboratory scale experiments can be crucial in knowing how mixed particle sizes travel. This study includes few set of preliminary results of particle size distribution within fracture. Extending this study to multiple experiments can provide information effect of particle uniformity and size distribution on proppant transport.

6.4. MULTIPLE PROPPANT SIZES

Scope of future studies can extend to use of proppant in multiple sizes. Using different sizes of proppant stage wise i.e. for example of injection of 40/70, followed by 30/50 proppant size. This performance should be evaluated through both laboratory scale experiments and simulations.

6.5. USING DIFFERENT FLUIDS WITH CURRENT APPROACH

Using fluids with different viscosity and flow properties should be used with current approach in order to understand the flow behaviour of proppant particles. The difference in proppant transport observed in fluids with different viscosity can be compared to results in this study.

APPENDIX

A.1. DIGITIZATION AND MEASUREMENT OF HEIGHTS

Measurements made manually for bed heights were verified by digitization of photograph captured at the end of each FPV. The image was transformed into coordinates of x and y which can be easily used to represent the height and distance to which the proppant has travelled in the fracture slot. The method to digitize an image is presented below using Figure A.1.

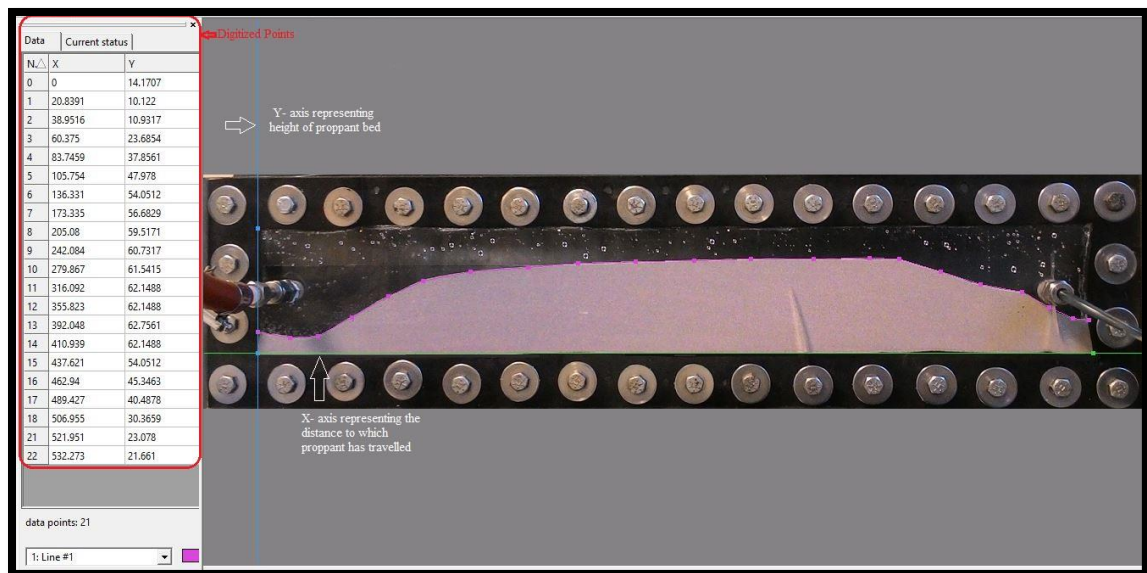


Figure A.1 Method to digitize the photo

Method to digitize an image using the plot digitizer

- Identify the origin and determine the x-axis and y-axis
- Provide the minimum and maximum value for each axis
- Click on each of the desired point on the image to get the coordinate value

- Coordinates of each of these points are obtained in a Table in the form of x and y where x represents the distance and y represent the height of proppant bed
- This procedure is repeated to obtain proppant travelled distance and bed heights at the end of each FPV

A.2. MEASURING PROPPANT SURFACE AREA

After obtaining the coordinates of desired points at the end of each FPV, the data was transferred on to a excel sheet. It is saved in alternate columns of X (representing distance) and Y (representing heights) of proppant bed. MATLAB code using the trapezoidal rule was used to calculate the area of proppant occupied area. To calculate the area, 2 steps have to be followed

- Please ensure that the data transferred on the excel sheet is presented in alternating columns of X and Y without any blank columns
- Enter the accurate File Name and Sheet Name in the first line of the code.
- Click on “Run” on “EDITOR” ribbon on MATLAB
- Area under curve will be calculated for each FPV in the selected sheet

The code is as below

```
runs = xlsread('FILE NAME','SHEET NAME');
% Store the number of columns of values in the sheet
[~,cols] = size(runs);
% preallocating a matrix to store the area
area_vec = zeros(cols/2,1);
```

```
% Iterating through all the x,y columns in the excel sheet to find the area
for i = 0:(cols/2)-1

Xval = runs(:,2*i+1);

% removing the NaN values that occur in the data
Xval(isnan(Xval)) = 0;

Yval = runs(:,2*i+2);

% removing the NaN values that occur in the data
Yval(isnan(Yval)) = 0;

% finding the area using the inbuilt trapz() function
area_vec(i+1) = trapz(Xval,Yval);

end

format long

uint64(area_vec)
```

REFERENCES

1. Alotaibi, M. A., & Miskimins, J. L. (2015, September 28). Slickwater Proppant Transport in Complex Fractures: New Experimental Findings & Scalable Correlation. Society of Petroleum Engineers. doi:10.2118/174828-MS.
2. Babcock, R. E., Prokop, C. L., & Kehle, R. O. (1967, January 1). Distribution of propping Agent in vertical Fractures. American Petroleum Institute.
3. Blyton, C. A. J., Gala, D. P., & Sharma, M. M. (2015, September 28). A Comprehensive Study of Proppant Transport in a Hydraulic Fracture. Society of Petroleum Engineers. doi:10.2118/174973-MS.
4. Clark, P. E. (2006, January 1). Transport of Proppant in Hydraulic Fractures. Society of Petroleum Engineers. doi:10.2118/103167-MS.
5. Clark, P. E., & Guler, N. (1983, January 1). Prop Transport in Vertical Fractures: Settling Velocity Correlations. Society of Petroleum Engineers. doi:10.2118/11636-MS.
6. Cinco L., H., Samaniego V., F., & Dominguez A., N. (1978, August 1). Transient Pressure Behavior for a Well With a Finite-Conductivity Vertical Fracture. Society of Petroleum Engineers. doi:10.2118/6014-PA.
7. Dayan, A., Stracener, S. M., & Clark, P. E. (2009, January 1). Proppant Transport in Slickwater Fracturing of Shale Gas Formations. Society of Petroleum Engineers. doi:10.2118/125068-MS.
8. Feng Liang, Mohammed Sayed, Ghaithan A. Al-Muntasheri, Frank F. Chang, Leiming Li, A comprehensive review on proppant technologies, *Petroleum*, Volume 2, Issue 1, 2016, Pages 26-39, ISSN 2405-6561, <http://dx.doi.org/10.1016/j.petlm.2015.11.001>.
9. Mack, M., Sun, J., & Khadilkar, C. (2014, February 4). Quantifying Proppant Transport in Thin Fluids: Theory and Experiments. Society of Petroleum Engineers. doi:10.2118/168637-MS.
10. Novotny, E. J. (1977, January 1). Proppant Transport. Society of Petroleum Engineers. doi:10.2118/6813-MS.
11. Gadde, P. B., Liu, Y., Norman, J., Bonnecaze, R., & Sharma, M. M. (2004, January 1). Modeling Proppant Settling in Water-Fracs. Society of Petroleum Engineers. doi:10.2118/89875-MS.

12. Han, J., Yuan, P., Huang, X., Zhang, H., Sookprasong, A., Li, C., & Dai, Y. (2016, May 5). Numerical Study of Proppant Transport in Complex Fracture Geometry. Society of Petroleum Engineers. doi:10.2118/180243-MS.
13. Hannah, R. R., & Harrington, L. J. (1981, May 1). Measurement of Dynamic Proppant Fall Rates in Fracturing Gels Using a Concentric Cylinder Tester (includes associated paper 9970). Society of Petroleum Engineers. doi:10.2118/7571-PA.
14. Jain, S., Soliman, M., Bokane, A., Crespo, F., Deshpande, Y., Kunnath Aven, N., & Cortez, J. (2013, February 4). Proppant Distribution in Multistage Hydraulic Fractured Wells: A Large-Scale Inside-Casing Investigation. Society of Petroleum Engineers. doi:10.2118/163856-MS.
15. Jones, J., & Britt, L. K. (2009). Design and Appraisal of Hydraulic Fractures. Richardson, Texas: Society of Petroleum Engineers. Retrieved from <http://store.spe.org/Design-and-Appraisal-of-Hydraulic-Fractures-P17.aspx>.
16. Kern, L. R., Perkins, T. K., & Wyant, R. E. (1959, July 1). The Mechanics of Sand Movement in Fracturing. Society of Petroleum Engineers. doi:10.2118/1108.
17. Kadhim, D., Imqam, A., & Dunn-Norman, S. (2017, July 24). Ceramic Proppant Transport and Placement in Heterogeneous Fracture Systems. Unconventional Resources Technology Conference.
18. Li, N., Li, J., Zhao, L., Luo, Z., Liu, P., & Guo, Y. (2016, August 24). Laboratory Testing and Numeric Simulation on Laws of Proppant Transport in Complex Fracture Systems. Society of Petroleum Engineers. doi:10.2118/181822-MS.
19. Liu, Y., & Sharma, M. M. (2005, January 1). Effect of Fracture Width and Fluid Rheology on Proppant Settling and Retardation: An Experimental Study. Society of Petroleum Engineers. doi:10.2118/96208-MS.
20. N.A. Patankar, D.D. Joseph, J. Wang, R.D. Barree, M. Conway, M. Asadi, Power law correlations for sediment transport in pressure driven channel flows, International Journal of Multiphase Flow, Volume 28, Issue 8, August 2002, Pages 1269-1292, ISSN 0301-9322, [http://dx.doi.org/10.1016/S0301-9322\(02\)00030-7](http://dx.doi.org/10.1016/S0301-9322(02)00030-7).
21. Palisch, T. T., Vincent, M. C., & Handren, P. J. (2008, January 1). Slickwater Fracturing Food for Thought. Society of Petroleum Engineers. doi:10.2118/115766-MS.
22. Sahai, R., Miskimins, J. L., & Olson, K. E. (2014, February 4). Laboratory Results of Proppant Transport in Complex Fracture Systems. Society of Petroleum Engineers. doi:10.2118/168579-MS.

23. Schmidt, D., Rankin, P. E. R., Williams, B., Palisch, T., & Kullman, J. (2014, February 4). The performance of Mixed Proppant Sizes. Society of Petroleum Engineers. doi:10.2118/168629-MS.
24. Schols, R. S., & Visser, W. (1974, January 1). Proppant Bank Buildup in a Vertical Fracture Without Fluid Loss. Society of Petroleum Engineers. doi:10.2118/4834-MS.
25. Songyang Tong, Kishore K. Mohanty, Proppant transport study in fractures with intersections, Fuel, Volume 181, 1 October 2016, Pages 463-477, ISSN 0016-2361.
26. Saldungaray, P. M., & Palisch, T. T. (2012, January 1). Hydraulic Fracture Optimization in Unconventional Reservoirs. Society of Petroleum Engineers. doi:10.2118/151128-MS.
27. Wang, J. Y., Holditch, S. A., & McVay, D. (2009, January 1). Modeling Fracture Fluid Cleanup in Tight Gas Wells. Society of Petroleum Engineers. doi:10.2118/119624-MS.
28. King, G. E. (2010, January 1). Thirty Years of Gas Shale Fracturing: What Have We Learned? Society of Petroleum Engineers. doi:10.2118/133456-MS.
29. Valko, P., & Economides, M. J. (1997, November 1). Foam Proppant Transport. Society of Petroleum Engineers. doi:10.2118/27897-PA.
30. Boyer, J., Maley, D., & O'Neil, B. (2014, October 27). Chemically Enhanced Proppant Transport. Society of Petroleum Engineers. doi:10.2118/170640-MS.
31. Harris, P. C., Walters, H. G., & Bryant, J. (2008, January 1). Prediction of Proppant Transport from Rheological Data. Society of Petroleum Engineers. doi:10.2118/115298-MS.
32. Harris, P. C., Morgan, R. G., & Heath, S. J. (2005, January 1). Measurement of Proppant Transport of Frac Fluids. Society of Petroleum Engineers. doi:10.2118/95287-MS.
33. Denney, D. (2010, October 1). Proppant Transport in Slickwater Fracturing of Shale-Gas Formations. Society of Petroleum Engineers. doi:10.2118/1010-0056-JPT
34. Walters, H. G., Stegent, N. A., & Harris, P. C. (2009, January 1). New Frac Fluid Provides Excellent Proppant Transport and High Conductivity. Society of Petroleum Engineers. doi:10.2118/119380-MS.

35. Roy, P., du Frane, W. L., & Walsh, S. D. C. (2015, November 13). Proppant Transport at the Fracture Scale: Simulation and Experiment. American Rock Mechanics Association.
36. Gruesbeck, C., & Collins, R. E. (1982, December 1). Particle Transport through Perforations. Society of Petroleum Engineers. doi:10.2118/7006-PA.

VITA

Vivekvardhan Reddy Kesireddy was born in Hyderabad, India. He received his bachelor's degree in Applied Petroleum Engineering from University of Petroleum and Energy Studies, India in 2013. He joined Tata Consultancy Services, India in July 2013 – July 2015 as a Drilling and Completions support Analyst. In August 2015, Vivek commenced his graduate studies in Petroleum Engineering at Missouri University of Science and Technology under Dr. Shari Dunn-Norman. During his time as a Master's Student, he held positions of Graduate Research Assistant in the department. He received his Master of Science degree in Petroleum Engineering from Missouri University of Science and Technology in December 2017.